



HAL
open science

Abiotic degradation of highly branched isoprenoid alkenes and other lipids in the water column off East Antarctica

Jean-Francois Rontani, Lukas Smik, Simon Belt, Frederic Vaultier, Linda Armbrrecht, Amy Leventer, Leanne Armand

► **To cite this version:**

Jean-Francois Rontani, Lukas Smik, Simon Belt, Frederic Vaultier, Linda Armbrrecht, et al.. Abiotic degradation of highly branched isoprenoid alkenes and other lipids in the water column off East Antarctica. *Marine Chemistry*, 2019, 210, pp.34-47. 10.1016/j.marchem.2019.02.004 . hal-02325661

HAL Id: hal-02325661

<https://hal.science/hal-02325661>

Submitted on 22 Oct 2021

HAL is a multi-disciplinary open access archive for the deposit and dissemination of scientific research documents, whether they are published or not. The documents may come from teaching and research institutions in France or abroad, or from public or private research centers.

L'archive ouverte pluridisciplinaire **HAL**, est destinée au dépôt et à la diffusion de documents scientifiques de niveau recherche, publiés ou non, émanant des établissements d'enseignement et de recherche français ou étrangers, des laboratoires publics ou privés.



Distributed under a Creative Commons Attribution - NonCommercial 4.0 International License

1 Abiotic degradation of highly branched isoprenoid alkenes
2 and other lipids in the water column off East Antarctica

3
4 Jean-François Rontani^{a,*}, Lukas Smik^b, Simon T. Belt^b, Frédéric Vaultier^a, Linda
5 Armbrecht^c, Amy Leventer^d, Leanne K. Armand^e

6
7 ^a Aix Marseille Université, Université de Toulon, CNRS/INSU/IRD, Mediterranean Institute of
8 Oceanography (MIO), UM 110, 13288 Marseille, France

9 ^b Biogeochemistry Research Centre, School of Geography, Earth and Environmental Sciences,
10 University of Plymouth, Drake Circus, Plymouth, Devon PL4 8AA, UK

11 ^c Australian Centre for Ancient DNA, School of Biological Sciences, Faculty of Sciences, The
12 University of Adelaide, Adelaide, South Australia, 5005, Australia

13 ^d Department of Geology, Colgate University, Hamilton, NY 13346, USA

14 ^e Research School of Earth Sciences, The Australian National University, Acton, Australian Capital
15 Territory, 2601, Australia.

16
17
18
19
20
21
22 * Corresponding author. Tel.: +33-4-86-09-06-02; fax: +33-4-91-82-96-41. *E-mail address:*
23 jean-francois.rontani@mio.osupytheas.fr (J.-F. Rontani)

26 **Abstract.** In some previous studies, the ratio between a di-unsaturated highly branched
27 isoprenoid (HBI) lipid termed IPSO₂₅ and a structurally related tri-unsaturated counterpart
28 (HBI III) (viz. IPSO₂₅/HBI III) has been used as a proxy measure of variable sea ice cover in
29 the Antarctic owing to their production by certain sea ice algae and open water diatoms,
30 respectively. To investigate this further, we quantified selected lipids and their photo- and
31 autoxidation products in samples of suspended particulate matter (SPM) collected at different
32 water depths in the polynya region west of the Dalton Iceberg Tongue (East Antarctica). The
33 results obtained confirm the high efficiency of photo- and autoxidation processes in diatoms
34 from the region. The systematic increase of the ratio IPSO₂₅/HBI III with water depth in the
35 current samples appeared to be dependent on the sampling site and was due to both (i) a
36 relatively higher contribution of ice algae to the deeper samples resulting from their increased
37 aggregation and therefore higher sinking rate, or (ii) a stronger abiotic degradation of HBI III
38 during settling through the water column. Analyses of samples taken from the water-sediment
39 interface and some underlying near-surface sediments revealed a further increase of the ratio
40 IPSO₂₅/HBI III, indicative of further differential oxidation of the more unsaturated HBI.
41 Unfortunately, specific oxidation products of HBI III could not be detected in the strongly
42 oxidized SPM and sediment samples, likely due to their lability towards further oxidation. In
43 contrast, oxidation products of HBI III were detected in weakly oxidized samples of
44 phytoplanktonic cells collected from Commonwealth Bay (also East Antarctica), thus
45 providing more direct evidence for the involvement of photo- and/or autoxidation of HBI III
46 in the region. This oxidative alteration of the ratio IPSO₂₅/HBI III between their source and
47 sedimentary environments might need to be considered more carefully when using this
48 parameter for palaeo sea ice reconstruction purposes in the Antarctic.

49

50

- 51 **Key words:** East Antarctica; Suspended particulate matter; Near-surface sediments; Lipids;
- 52 Photo- and autoxidation; Alteration of IPSO₂₅/HBI III ratio; Paleoceanographic implications.

53 **1. Introduction**

54 Sea ice plays a central role in the overall climate structure of the Polar Regions
55 (Thomas, 2017). Amongst its various well known attributes, its high albedo (reflectivity)
56 means that sea ice serves as an efficient regulator of incoming solar radiation to the surface
57 oceans. Further, the physical structure of sea ice provides a physical barrier to the
58 exchange of gas, heat and moisture between the polar oceans and the atmosphere. It is also
59 an important contributor to near-surface stratification, bottom-water formation and
60 ventilation, in particular (e.g. Dickson et al., 2007 and references therein). From a
61 biogeochemical perspective, nutrient release during ice melt in spring, coupled with
62 surface layer stratification and increasing light and temperature, often leads to intense open
63 water phytoplankton production, especially along the retreating ice edge or the so-called
64 marginal ice zone (MIZ) (Smith and Nelson 1986; Smith, 1987; Sakshaug et al., 2009;
65 Perette et al., 2011).

66 Understanding the well documented abrupt changes in sea ice in the polar regions
67 (Stroeve et al., 2012; Fetterer et al., 2016, Serreze et al., 2016; Walsh et al., 2017) requires
68 more detailed knowledge of how it has changed in the past in response to other climatic
69 drivers. A common approach to achieve this is through the analysis of so-called sea ice
70 proxies present in marine sediment archives. The majority of these proxies possess some
71 kind of biological origin, although there are others (e.g. de Vernal et al., 2013 and
72 references therein). In the Antarctic, the identification of certain ice-associated diatoms in
73 polar marine sediments has a long history of use for palaeo sea ice determinations (Armand
74 et al., 2017). However, the growth habitat of the target species are normally more closely
75 associated with the open waters of the MIZ rather than that of sea ice itself (Leventer,
76 1998; Leventer et al., 2008). On the other hand, those diatoms that bloom within the sea ice

77 host (i.e. the strictly sympagic community), are often under-represented in sedimentary
78 records (Leventer, 2013).

79 Over the last decade or so, a number of diatom-derived lipid biomarkers have
80 emerged as useful complementary sea ice proxies to the more traditional
81 micropaleontological-based approaches. Thus a mono-unsaturated highly branched
82 isoprenoid (HBI) termed IP₂₅ (Ice Proxy with 25 carbon atoms; Belt et al., 2007) has
83 emerged as a useful proxy for seasonal Arctic sea ice (for reviews, see Belt and Muller,
84 2013; Belt, 2018), while a di-unsaturated structural homolog of IP₂₅ – sometimes referred
85 to as HBI II (**1**; see appendix) – appears to be a suitable counterpart for the Antarctic. A
86 recent source identification and the near ubiquity of the diene **1** in near-coastal sediments
87 from around the Antarctic continent has led to its recent designation as IPSO₂₅ (Ice Proxy
88 for the Southern Ocean with 25 carbon atoms; Belt et al., 2016) by analogy with IP₂₅. A
89 further, tri-unsaturated HBI, often termed HBI III (**2**), is also showing potentially as a
90 biomarker proxy indicator of the MIZ in both Polar Regions. Thus, enhanced
91 concentrations of HBI III (**2**) have been observed in surface sediments from the MIZ of the
92 Barents Sea in the Arctic (Belt et al., 2015) and in surface waters of the MIZ in East
93 Antarctica (Smik et al., 2016) and the Scotia Sea (Schmidt et al., 2018) shortly following
94 sea ice melt. As a result, some palaeo sea ice records based on HBI II (hereafter referred to
95 as IPSO₂₅) (**1**) and HBI III (**2**) for the Antarctic have appeared in recent years (Barbara et
96 al., 2010,2013,2016; Denis et al., 2010; Collins et al., 2013; Etourneau et al., 2013;
97 Campagne et al., 2015,2016). A general interpretation of greater sea ice extent for
98 relatively high IPSO₂₅ (**1**) compared to HBI III (**2**), and more open water conditions for
99 increased HBI III (**2**) concentrations has been applied. In some of these studies, variability
100 in the ratio **1/2** has been used as a qualitative measure of changes to sea ice cover;
101 however, this assumption has, as yet, not been validated through comparison of surface

102 sediment biomarker data with known overlying sea ice conditions in the same way as for
103 IP₂₅ (and HBI III (2) in some cases) in the Arctic (see Belt, 2018 for a recent review).
104 Nonetheless, such interpretations are consistent with the data reported by Smik et al.
105 (2016) following analysis of IPSO₂₅ (1) and HBI III (2) in surface waters from regions of
106 variable sea ice cover from East Antarctica, with highest concentrations found in the
107 summer sea ice zone and MIZ, respectively. Similar findings have also been reported for
108 surface water samples from the Scotia Sea (Schmidt et al., 2018). However, the extent to
109 which the surface water distributions of IPSO₂₅ (1) and HBI III (2) are replicated in the
110 underlying sediments for palaeo sea ice reconstruction purposes was not investigated in the
111 initial study by Smik et al. (2016).

112 To provide further insight to this, here we carried out analysis of further water
113 samples from the polynya region proximal to the Dalton Ice Tongue in East Antarctica
114 with the primary aim of determining any variability of the ratio **1/2** with water depth, and
115 to reconcile outcomes through the identification of pathway-specific oxidation products of
116 common phytoplankton lipids as indicators of well-known degradation processes (i.e.
117 bacterial degradation, photooxidation and autoxidation). Further evidence for the oxidation
118 of such lipids was obtained through the analysis of near-surface sediment material
119 collected from the main study region and from filtered phytoplankton samples collected
120 from Commonwealth Bay (also East Antarctica).

121

122 **2. Materials and methods**

123

124 *2.1. Sampling*

125 Water samples were obtained as part of the NBP1402 cruise aboard the RVIB
126 *Nathaniel B Palmer* in February–March 2014 as described previously (Smik et al., 2016;

127 see also NBP1402 Scientific Cruise Report, 2014, Sabrina Coast: Marine record of
128 cryosphere–ocean dynamics (467 pages) for further details)
129 (http://www.marinegeo.org/tools/search/data/field/NBPalmer/NBP1402/docs/NBP1402CruiseReport_Final.pdf). For the current study, we focused on those locations that had
130 experienced seasonal sea ice cover within the polynya region west of the Dalton Iceberg
131 Tongue (East Antarctica). At each of the 12 sampling sites (Fig. 1), surface (0–10 m), sub-
132 surface (chlorophyll *a* maximum; ca. 25–60 m) and deep (ca. 500–1100 m) water samples
133 were obtained from CTD rosettes. At the five stations where we carried out lipid
134 degradation studies, the surface CTD samples had already been used for native lipid
135 analyses so we used water obtained from the ship’s intake line (ca. <10 m); near-surface
136 and deep water samples were obtained from the CTD rosettes as per the other stations. In
137 each case, 1.5–3.0 l of sampled water was filtered onto 25 mm Whatman GF/F filters (as
138 supplied), wrapped in aluminium foil and stored frozen (-80°C). Sample data are detailed
139 in Supplementary Table 1. Megacoring was conducted using a Bowers and Connelly
140 MegaCorer, with 12 10-cm diameter core tubes, for sampling an undisturbed sediment
141 water interface. Surface water above the core tops and a layer of diatomaceous ‘fluff’ were
142 pipetted off the top of the core tubes and stored frozen (-80°C). Sediment material from the
143 cores was extruded at 0.5 to 2 cm intervals, depending on the core depth.

145 Three samples of phytoplankton cells (CB, AS607 and AS608) were collected in
146 Commonwealth Bay (East Antarctica, 66°56S; 142°27E) during the IPEV-COCA2012
147 cruise in January 2012. Surface waters were sampled using a 25- μ m ring net deployed
148 from the R/V Astrolabe. Concentrated phytoplankton cell suspensions (ranging from 2.6 to
149 1.1 mg d.w. ml⁻¹) were stored frozen (-20 °C) prior to freeze drying and analysis.

150

151 *2.2. Sample treatment*

152 Lipids from all of the CTD samples, the waters above the sediment cores and the
153 diatomaceous ‘fluff’ were extracted and analyzed as described previously by Smik et al.
154 (2016). This treatment involved addition of internal standards (9-octyl-8-heptadecene for
155 HBI quantification, 5 α -androstan-3 β -ol for Δ^5 -sterol quantification and nonadecanoic acid
156 for fatty acid quantification), saponification (5% KOH (9:1 v/v MeOH/H₂O); 70 °C; 60
157 min) and separation of non-saponifiable (hexane 3x2 ml) and saponifiable fractions (+1 ml
158 HCl; hexane (3x2 ml)). For sediments, ca. 1 g of freeze-dried material was extracted by
159 sonication (dichloromethane/methanol; 2:1 v/v, 3x2 ml) to obtain a total organic extract
160 (TOE). Subsequent purification of the unsaponifiable fraction/TOE by open column
161 chromatography (SiO₂) afforded HBIs (elution with hexane; 5 column volumes) and
162 sterols (elution with hexane-methyl acetate (4:1, v/v; 5 column volumes). In addition,
163 saturated non-polar components of TOEs were removed using silver-ion chromatography
164 (Belt et al., 2015).

165 Treatment of the filtered water samples from the five stations selected for lipid
166 oxidation product analyses and phytoplankton material collected from Commonwealth Bay
167 involved a different treatment. Following addition of MeOH (25 ml) and reduction with
168 excess NaBH₄ (70 mg, 30 min) of labile hydroperoxides to alcohols, which are more
169 amenable to analysis using gas chromatography–mass spectrometry (GC-MS), water (25
170 ml) and KOH (2.8 g) were added and the resulting mixture saponified by refluxing (2 h).
171 After cooling, the mixture was acidified (HCl, 2 N) to pH 1 and extracted with
172 dichloromethane (DCM; 3 x 20 ml). The combined DCM extracts were dried over
173 anhydrous sodium sulfate, filtered and concentrated via rotary evaporation at 40°C to give
174 total lipid extracts (TLEs).

175 A different treatment (Rontani et al., 2018) was employed to estimate the relative
176 proportions of hydroperoxides and their ketonic and alcoholic degradation products in

177 phytoplankton samples from Commonwealth Bay. This involved ultrasonic extraction of
178 lipids with chloroform-MeOH-water (1:2:0.8, v/v/v), separation of the supernatant by
179 centrifugation at 3500G, evaporation to dryness, and division of the residue into two equal
180 parts. The first sub-sample was acetylated in acetic anhydride-pyridine (1:2, v/v) overnight,
181 which converted hydroperoxides to the corresponding ketones (Mihara and Tateba, 1986),
182 and then saponified. The second sub-sample was reduced with NaBD₄ and saponified.
183 Comparison of the amounts of alcohols present after acetylation and NaBD₄ reduction
184 made it possible to estimate the amount of hydroperoxides and alcohols present in the
185 samples, while deuterium labeling (via NaBD₄ reduction) allowed us to estimate the
186 proportion of ketones in the samples.

187

188 *2.3. Derivatization*

189 For all samples containing hydroxylic components, an aliquot was dissolved in 300
190 µl pyridine/bis(trimethylsilyl)trifluoroacetamide (BSTFA, Supelco; 2:1, v:v) and silylated
191 (1 h) at 50 °C. After evaporation to dryness under a stream of N₂, the derivatized residue
192 was dissolved in a mixture of ethyl acetate and BSTFA (to avoid desilylation) and
193 analyzed by GC-MS, GC-QTOF or GC-MS/MS.

194

195 *2.4. Assignment and quantification of lipids*

196 Native lipids were identified and quantified using GC-MS in total ion current (TIC)
197 or selected ion monitoring (SIM) mode using a Hewlett-Packard 5890 Series II gas
198 chromatograph, fitted with a 30 m fused silica HP_{5ms} column (0.25 mm i.d., 0.25 µm film)
199 coupled to a 5970 Series Mass Selective Detector (MSD) (Belt et al., 2012). Individual
200 lipids (and their derivatised products) were identified on the basis of their characteristic
201 GC retention indices (e.g. RI_{HP5ms} 2082 and 2044 for IPSO₂₅ and HBI III, respectively) and

202 mass spectra (Belt, 2018), together with comparison of both parameters with those
203 obtained from purified standards (Smik et al., 2016). Quantification of individual lipids
204 was achieved first by manual integration of GC–MS peak areas, division of these by those
205 of the respective internal standards, and normalization of the resulting ratios using
206 instrumental response factors obtained for each lipid (Belt et al., 2014; Smik et al., 2016).
207 These normalised ratios were then multiplied by the mass of the internal standard and
208 finally converted to their corresponding seawater concentrations using the volume of water
209 filtered or mass of sediment extracted. All analytical data can be found in Supplementary
210 Table 1.

211

212 *2.5. Assignment and quantification of lipid oxidation products*

213 Lipid oxidation products were identified by comparison of retention times, accurate
214 masses and mass spectra with those of standards and quantified (calibration with external
215 standards) using gas chromatography–electron ionization quadrupole time of flight mass
216 spectrometry (GC-QTOF). GC-QTOF analyses were carried out with an Agilent
217 7890B/7200A GC-QTOF System (Agilent Technologies, Parc Technopolis - ZA
218 Courtaboeuf, Les Ulis, France). A cross-linked 5% phenyl-methylpolysiloxane (Macherey
219 Nagel; Optima 5-MS Accent) column (30 m × 0.25 mm, 0.25 µm film thickness) was
220 employed. Analyses were performed with an injector operating in pulsed splitless mode at
221 280 °C and the oven temperature programmed from 70 °C to 130 °C at 20 °C min⁻¹, then to
222 250 °C at 5 °C min⁻¹, and then to 300 °C at 3 °C min⁻¹. The carrier gas (He) was
223 maintained at 0.69 × 10⁵ Pa until the end of the temperature program. Instrument
224 temperatures were 300 °C for the transfer line and 230 °C for the ion source. Accurate
225 mass spectra were obtained across the range *m/z* 50-700 at 4 GHz. The QTOF-MS

226 instrument provided a typical resolution ranging from 8009 to 12252 from m/z 68.9955 to
227 501.9706. Perfluorotributylamine (PFTBA) was utilized for daily MS calibration.

228

229 *2.6. Assignment and quantification of HBI oxidation products*

230 Quantification of HBI oxidation products was carried out using an Agilent 7850-A
231 gas chromatograph connected to an Agilent 7010-QQQ mass spectrometer working in
232 multiple reaction monitoring (MRM) mode. The following conditions were employed: 30
233 m x 0.25 mm (i.d.) fused silica column coated with HP-5MS (Agilent; film thickness: 0.25
234 μm); oven programmed from 70 to 130 $^{\circ}\text{C}$ at 20 $^{\circ}\text{C min}^{-1}$, then to 250 $^{\circ}\text{C}$ at 5 $^{\circ}\text{C min}^{-1}$ and
235 then to 300 $^{\circ}\text{C}$ at 3 $^{\circ}\text{C min}^{-1}$; carrier gas (He), 1.0 bar; injector (splitless), 250 $^{\circ}\text{C}$; electron
236 energy, 70 eV; source temperature, 230 $^{\circ}\text{C}$; quadrupole temperature, 150 $^{\circ}\text{C}$; scan range
237 m/z 40-700; collision energy, ranging from 5 to 15 eV; collision flow, 1.5 ml min^{-1} (N_2);
238 quench flow, 2.25 ml min^{-1} (He); cycle time, 0.2 s. Oxidation products were assigned by
239 comparison of retention times and mass spectra with those of standards. Due to the
240 presence of two highly photo-reactive tri-substituted double bonds (C-7/20 and C-9/10) in
241 HBI III (**2**), it was not possible to quantify its primary oxidation products directly using
242 standards, since they are not accumulated due to rapid further oxidation (Rontani et al.,
243 2014a). We therefore quantified photoproducts of a related HBI triene (**3**) (possessing only
244 one reactive tri-substituted double bond (C-9/10); see appendix) as an external standard
245 and estimated the quantities of oxidation products from HBI III (**2**) by applying a
246 correction factor (Rontani et al., 2014b).

247

248 *2.7. Standard compounds*

249 The synthesis of 3-methylidene-7,11,15-trimethylhexadecan-1,2-diol (phytyldiol) (**7**)
250 was described previously by Rontani and Aubert (2005). (8-11)-Hydroperoxyhexadec-(8-

251 10)-enoic acids (*Z* and *E*) (**36-41**) and (8-11)-Hydroperoxyoctadec-(8-10)-enoic (*Z* and *E*)
252 (**30-35**) acids were produced by Fe²⁺/ascorbate-induced autoxidation (Loidl-Stahlhofen and
253 Spiteller, 1994) of palmitoleic and oleic acids, respectively. Subsequent reduction of these
254 different hydroperoxides in methanol with excess NaBH₄ afforded the corresponding
255 hydroxyacids. 3,6-Dihydroxy-cholest-4-ene (**18**) (employed for sterol photooxidation
256 estimates) was obtained from Maybridge Ltd. Treatment of sitosterol (**42**) with meta-
257 chloroperoxy-benzoic acid in dry DCM yielded a mixture of 5 α ,6 α -and 5 β ,6 β -epoxides.
258 Heating of these epoxides in the presence of water afforded the corresponding 24-
259 ethylcholesta-3 β ,5 α ,6 β -triol (**43**) (Holland and Diakow, 1979). IPSO₂₅ (**1**) and HBI triene
260 **3** were purified from cultures of *Haslea ostrearia* (Belt et al., 1996; Johns et al., 1999),
261 while HBI III (**2**) was obtained from a culture of *Pleurosigma intermedium* (Belt et al.,
262 2000). Photosensitized oxidation products (hydroperoxides) of these HBI alkenes were
263 produced in pyridine in the presence of haematoporphyrin as photosensitizer and then
264 reduced with NaBH₄ to the corresponding alcohols (Rontani et al., 2014a).

265

266 2.8 *Diatom taxonomy*

267 Diatom identification and enumeration were carried out for selected water and
268 sediment samples. Specifically, three water samples of 200 ml each were collected at
269 CTD015 (5, 40, 563 m). Overlying bottom water (100 μ l), diatomaceous fluff (50 μ l) and
270 sediment samples were collected from MC061. Sediment was also collected from MC045.
271 The water samples were immediately fixed with Lugol's solution (~0.5 ml). Back at the
272 laboratory, the preserved water samples were concentrated (CTD015) or diluted (MC061)
273 into Utermöhl chambers to a final volume of 3 ml. After sedimentation of 48 h, a minimum
274 total of 400 cells (including microphyto- and microzooplankton live at the time of
275 preservation), were identified and counted following the Utermöhl method (Utermöhl,

276 1958) at a magnification of 400x under an inverted microscope (Olympus IMT-2, Japan).
277 Microplankton were identified to species level where possible using appropriate taxonomic
278 literature (Hasle, 1965; Tomas, 1997; Scott and Marchant, 2005, Kim et al. 2013). Final
279 counts were converted to cells l⁻¹. Sediment samples were dried at 50 °C. Quantitative
280 slides were made using a settling method (Scherer, 1994). Approximately 5 ml of water
281 and hydrogen peroxide was added to several mg of each sample, and the samples were
282 placed on a warming tray at 50 °C for 2–3 days. After complete reaction and removal of
283 organic material, the samples were poured into water-filled 1 l beakers and allowed to
284 settle onto coverslips. The coverslips were mounted on glass slides using Norland Optical
285 Adhesive #61 cured under UV light. These quantitative slides were used for assessment of
286 the diatom assemblage, by identification and counting of a minimum of 400 diatom valves
287 along cross-slide transects, at a magnification of 1000x. Counting followed the method
288 described by Schrader and Gersonde (1978) and Crosta and Koc (2007). Diatom
289 concentration (diatom valves per gram) and relative abundance (percentage) of diatom
290 species were calculated.

291 For the purposes of the current investigation, we determined the distribution of three
292 common *Fragilariopsis* spp. to provide a semi-quantitative assessment of the relative
293 contribution from sea ice-associated (*F. curta* and *F. cylindrus*) and open water (*F.*
294 *kerguelensis*) diatoms. (Armand et al., 2005; Crosta et al., 2005; Crosta et al., 2008). Thus,
295 the ratio (*F. curta* + *F. cylindrus*)/*F. kerguelensis* was determined (Table 2).

296

297 **3. Results and discussion**

298 The identification and quantification of the various lipids and their degradation
299 products are described here according to the individual lipid classes at each sampling
300 location. The sequence of presentation is arranged so as to first provide sufficient evidence

301 for the oxidation state of the lipids, in order that the variability in the ratio of IPSO₂₅
302 (1)/HBI III (2) can then be put into context.

303

304 *3.1. Lipids and their degradation products in water samples from west of the Dalton*

305 *Iceberg Tongue*

306

307 3.1.1. Chlorophyll phytol side-chain

308 In addition to phytol (4), which mainly arises from the hydrolysis of the chlorophyll
309 phytol side-chain during alkaline hydrolysis, significant amounts of 3,7,11,15-
310 tetramethylhexadecanoic acid (phytanic acid) (5), 3,7,11,15-tetramethylhexadec-1-en-ol-3
311 (isophytol) (6) and 3-methylidene-7,11,15-trimethylhexadecan-1,2-diol (phytyldiol) (7)
312 could also be detected in the different samples. However, phytanic acid (5) was not
313 quantified in the present work due to its lack of specificity. Indeed, this isoprenoid acid is
314 also formed during the aerobic and anaerobic bacterial degradation of phytol (Rontani and
315 Volkman, 2003) and the grazing of phytoplankton (Prahl et al., 1984).

316 In contrast, there have been very few reports of the presence of isophytol (6) in the
317 marine environment (Fang et al., 2006), so its relatively high proportion compared to
318 phytol (1) in some samples (Table 1) is potentially surprising. Isophytol (6) may be formed
319 in sediments either by enzyme-catalyzed allylic rearrangement during bacterial degradation
320 of phytol under denitrifying conditions (Rontani et al., 1999), or by clay-catalyzed
321 dehydration of phytol (de Leeuw et al., 1974). It is interesting to note that relatively high
322 proportions of isophytol were also recently observed after NaBH₄-reduction and alkaline
323 hydrolysis of phytoplanktonic cells collected from Commonwealth Bay, Antarctica
324 (Rontani and Galeron, 2016). In order to explain this observation, it was proposed that

allylation (Berkessel, 2009) of the chlorophyll phytyl side-chain by peroxy radicals could result in the formation of the precursor 3-peroxy-3,7,11,15-tetramethylhexadec-1-ene (**8**), with subsequent reduction to isophytol (**6**) (Fig. 2) (Rontani and Galeron, 2016). The absence of the initial reduction step employed here (i.e. using NaBH₄) during conventional treatment of environmental samples is likely at the origin of the very few reports of isophytol (**6**) in previous studies. In any case, the high values of the ratio isophytol/phytol observed at station 25, and to a lesser extent at station 28B (Table 1), attest to the presence of high concentrations of peroxides, and thus of a strong photo- or autoxidation state of POM.

The formation of phytyldiol (**7**) results from initial Type II photosensitized oxidation (i.e. involving singlet oxygen (¹O₂)) of the chlorophyll phytyl side-chain and subsequent hydrolysis of the photoproducts thus formed (Rontani et al., 1994). On the basis of its high specificity and widespread occurrence in the environment (Cuny and Rontani, 1999), this diol can be used as a specific tracer of chlorophyll photodegradation. Further, Cuny et al. (2002) proposed that the amount of chlorophyll photodegradation in the marine environment could be estimated from the so-called Chlorophyll Phytyl side-chain Photodegradation Index (CPPI) derived from the molar ratio phytyldiol/phytol. Using this approach, the highest photooxidation state of POM was confirmed as being at station 25 and the lowest at station 32 (<1%, not included in the figure) (Fig. 3).

344

3.1.2. Sterols

The major sterols in the filtered water sample were 24-norcholest-5,22*E*-dien-3β-ol (22-dehydrocholesterol) (**10**), cholest-5-en-3β-ol (cholesterol) (**11**), 24-methylcholesta-5,22*E*-dien-3β-ol (*epi*-brassicasterol) (**12**), 24-methylcholesta-5,24(28)-dien-3β-ol (24-methylenecholesterol) (**13**) and 24-ethylcholest-7-en-3β-ol (22-dihydrocondrillasterol) (**14**)

350 (Supplementary Table 1). 22-Dehydrocholesterol (**10**) has been found in diatoms and
351 notably in *Thalassiosira aff. antarctica* (Rampen et al., 2007). Although cholesterol (**11**)
352 may be derived from diatoms or Prymnesiophycean algae (Volkman, 1986), its dominance
353 generally suggests an important contribution of zooplanktonic faecal material to the
354 samples. Indeed, it is well known that zooplankton convert much of the sterols produced
355 by algae into cholesterol (**11**) (Volkman et al., 1980; Prahl et al., 1984). *Epi*-brassicasterol
356 (**12**) and 24-methylenecholesterol (**13**) are major constituents of several diatom species
357 (Lee et al., 1980) including sea ice diatoms (Belt et al., 2018). However, it may be noted
358 that *epi*-brassicasterol (**12**) is also present in some dinoflagellates and in many haptophytes
359 (Volkman, 1986, 2003). The unusual sterol 22-dihydrochondrillasterol (**14**) was detected
360 previously in some Chlorophyceae (Martin-Creuzburg et al., 2011; Martin-Creuzburg and
361 Merkel, 2016). The sterol profiles observed in these samples (Supplementary Table 1) are
362 thus typical of mixed assemblages of diatoms, Prymnesiophytes and Chlorophytes.

363 Type II photosensitized oxidation of Δ^5 -sterols produces mainly unstable Δ^6 -5 α -
364 hydroperoxides with low amounts of Δ^4 -6 α/β -hydroperoxides (Smith, 1981). Here, we
365 selected Δ^4 -6 α/β -hydroperoxides as tracers of photooxidation of Δ^5 -sterols due to their
366 high specificity and relative stability (Rontani et al., 2009; Christodoulou et al., 2009).
367 These compounds were quantified after NaBH₄ reduction to the corresponding diols and
368 photooxidation percentage was obtained from the equation: photooxidation % = (Δ^4 -stera-
369 6 α/β -diols % \times (1+0.3)/0.3) (Christodoulou et al., 2009). The values obtained for *epi*-
370 brassicasterol (**12**) and 24-methylenecholesterol (**13**) (the two main algal sterols present in
371 the samples analyzed) are shown in Fig. 3. Photooxidation of these two sterols exhibits the
372 same general trend as that seen for chlorophyll, with the highest photooxidation state
373 observed at station 25 (Fig. 3). Interestingly, as observed previously in the Arctic (Rontani
374 et al., 2012; 2014a), photodegradation processes appeared to have acted more intensively

375 on 24-methylenecholesterol (**13**) (mainly arising from diatoms) than on *epi*-brassicasterol
376 (**12**) (arising from diatoms and/or Prymnesiophytes). These differences confirm the higher
377 efficiency of Type II photosensitized oxidation processes in diatoms compared to
378 Prymnesiophytes.

379 Stanols constitute useful indicators of bacterial degradation of Δ^5 -sterols (Gagosian
380 et al., 1982; de Leeuw and Baas, 1986; Wakeham, 1989). We thus quantified the ratio 24-
381 methyl-5 α -cholest-22*E*-en-3 β -ol (*epi*-brassicastanol) (**15**)/*epi*-brassicasterol (**12**) to
382 indicate the extent of bacterial degradation of algal material. (Note: the ratio 24-methyl-
383 5 α -cholest-24(28)-en-3 β -ol (**16**)/24-methylenecholesterol (**13**) could not be quantified due
384 to co-elution of the stanol **16** with the isobaric campesterol (**17**)). The values of the ratio
385 *epi*-brassicastanol (**15**)/*epi*-brassicasterol (**12**) (Table 1) show only a weak increase with
386 depth suggesting that bacterial degradation processes acted only weakly on algal material.

387

388 3.1.3. Fatty acids

389 The fatty acid content of the SPM samples is characterized by a very low content of
390 polyunsaturated fatty acids (PUFAs) and notably of C_{18:4} (**19**), C_{20:5} (**20**) and C_{22:6} (**21**)
391 acids, which are typical for marine plankton (Kattner et al., 1983). Instead, the dominant
392 fatty acids are the saturated and monounsaturated fatty acids (MUFAs) (i.e. C_{14:0} (**22**),
393 C_{16:1 ω 7} (palmitoleic acid) (**23**), C_{16:0} (palmitic acid) (**24**), C_{18:1 ω 9} (oleic acid) (**25**), C_{18:1 ω 7}
394 (vaccenic acid) (**26**) and C_{18:0} (**27**)) (Supplementary Table 1). The reactivity of unsaturated
395 fatty acids with respect to auto- and photooxidative processes increases, logically, with the
396 number of double bonds (Frankel, 1998; Rontani et al., 1998). The very low amounts of
397 PUFAs is therefore suggestive of intense photo- or autooxidation of the samples. In order to
398 confirm this, the oxidation products of MUFAs (oleic and palmitoleic acids) (**25** and **23**)
399 were quantified since they are sufficiently stable in the marine environment to act as

400 markers of these abiotic degradative processes (Marchand and Rontani, 2001, 2003).
401 Photo- and autoxidation of monounsaturated fatty acids affords mixtures of isomeric allylic
402 hydroperoxyacids (Frankel, 1998). Based on the specific formation of *cis* isomers by
403 autoxidation (Porter et al., 1995), the relative importance of photooxidation and
404 autoxidation can easily be distinguished by quantifying the respective hydroxyacids that
405 result from NaBH₄-reduction of these compounds (Marchand and Rontani, 2001). The
406 results obtained (Fig. 4) show a clear difference in reactivity between palmitoleic (**23**) and
407 oleic (**25**) acids. Indeed, photo- and autoxidation states appeared to be considerably higher
408 in the case of palmitoleic acid (**23**) (the main MUFA of diatoms, Fahl and Kattner, 1993;
409 Leu et al., 2010) compared to oleic acid (**25**) (dominant in Prymnesiophytes, Rossi et al.,
410 2006). These outcomes are consistent with previous observations of more efficient photo-
411 and autoxidation processes in diatoms than in Prymnesiophytes (Rontani et al., 2012;
412 2014b). Such differences in reactivity were attributed previously to the involvement of
413 intra-cellular compartmentalization effects, which may significantly modify the reactivity
414 of lipids towards autoxidative and photooxidative processes according to their location in
415 phytoplanktonic cells (Rontani, 2012).

416 The palmitoleic (**23**)/palmitic acid (**24**) ratio is often employed to follow diatom
417 blooms (Pedersen et al., 1999; Reuss and Poulsen, 2002). Due to the strong oxidation of
418 palmitoleic acid (**23**) observed in some of our samples (Fig. 4), we employed the ratio (Σ
419 palmitoleic acid (**23**) and its oxidation products)/palmitic acid (**24**) to estimate the relative
420 proportion of diatom in the mixed phytoplankton assemblages. Using this approach, we
421 observed a relatively high proportion of (strongly oxidized) diatoms in the surface water
422 sample of station 25 and an increase in their proportion with water depth at station 28B
423 (Table 1).

424

425 3.1.4. Cutin components

426 Relatively high amounts of 9,16-dihydroxyhexadecanoic (**29**) and 10,16-
427 dihydroxyhexadecanoic (**28**) acids were observed in some samples (Table 1). These
428 compounds are well-known depolymerisation products of cutins (insoluble polyester
429 polymers) present in the outer layer of the epidermal cells of primary plant tissues, such as
430 leaves) (Deas and Holloway, 1977; Kolattukudy, 1977, 1980). The presence of such
431 compounds is very surprising since the Antarctic biome is an unfavorable environment for
432 higher plant growth. Only two native phanerogams, *Deschampsia antarctica* Desv. and
433 *Colobanthus quitensis* (Kunth) Bartl., occur in Antarctica to almost 69°S (Smith 1994).
434 The high concentrations of dihydroxyacids **28** and **29** detected in some sub-surface water
435 samples (Table 1) is therefore attributed to the accumulation of low density debris of such
436 plants, probably resulting from inflow of near-surface water masses carrying terrestrial
437 material. In contrast, the occurrence of these compounds due to sediment resuspension
438 seems unlikely due to their absence in the deeper water column samples.

439

440 3.1.5. HBI alkenes

441 The two HBI lipids, IPSO₂₅ (**1**) and HBI III (**2**), reported previously by Smik et al.
442 (2016) in the surface water samples described here, were also present in each of the sub-
443 surface and deep water samples investigated for the first time within the current study.
444 Although there was some variability in the absolute and relative concentrations of these
445 HBIs between the surface and sub-surface samples, The IPSO₂₅ (**1**)/HBI III (**2**) ratio was
446 mainly slightly higher in the majority of the sub-surface samples compared to the surface
447 water counterparts, with CTD-004 and -014 the only exceptions. More striking changes to
448 this ratio were observed with the corresponding deep water samples, however, with mean

449 (i.e. across all samples) relative enhancements in IPSO₂₅ (**1**)/HBI III (**2**) of ca. 8 and 6
450 when compared with the surface and sub-surface samples, respectively (Table 1).

451 The systematic increase of the ratio **1/2** with depth (Table 1) may potentially be
452 attributed to: (i) a relatively higher contribution of ice algae (and thus IPSO₂₅ (**1**)) to the
453 deeper samples resulting from their stronger aggregation and therefore higher sinking rate,
454 or (ii) a stronger abiotic degradation of HBI III (**2**) during settling through the water
455 column. One characteristic of sea ice algae is their ability to produce high amounts of
456 extracellular polymeric substances (EPS); the production of which facilitates the
457 attachment of algae to their substrate (sea ice) but also allows the formation of aggregates
458 of algal cells (Riebesell, 1991; Alldredge et al., 1993; Passow, 2002), thus shortening their
459 residence time within the euphotic zone. In the case of station 28B, the simultaneous
460 increase of the ratios **1/2** and (Σ palmitoleic acid (**23**) and its oxidation products)/palmitic
461 acid (**24**) with depth (Table 1) suggests a dominance of aggregated ice diatom material in
462 the deepest SPM sample.

463 Photo- and autoxidation of IPSO₂₅ (**1**) were previously studied in vitro (Rontani et
464 al., 2011; 2014a). Based on its very low degradation rates (resulting from the poor
465 reactivity of its two terminal double bonds (i.e. at C6-17 and C23-24) towards ¹O₂ and free
466 radicals), it is feasible that this diene (**1**) could be largely unaffected by abiotic oxidation
467 within the water column of the oceans, at least in comparison with some more unsaturated
468 lipids, or those containing more reactive double bonds. Indeed, HBI III (**2**) possesses two
469 tri-substituted double bonds (i.e. at C7–20 and C9–10), both of which are more reactive
470 towards ¹O₂ (Frimer, 1983) than the two double bonds in IPSO₂₅. In addition, the relative
471 positions of these two double bonds in HBI III (**2**) creates a bis-allylic methylene group (at
472 C-8) that can lose a hydrogen atom even more readily (Yin et al., 2011). HBI III (**2**) is thus
473 very sensitive towards photo- and autoxidation processes and exhibits degradation rates

474 close to those of PUFAs (Rontani et al., 2014a). On the basis of the very intense abiotic
475 alteration of these fatty acids in the samples investigated here (see section 3.1.3), a similar
476 oxidation of HBI III (**2**) was thus expected. However, we were not able to detect the
477 previously identified primary oxidation products of HBI III (**2**) (Rontani et al., 2014a),
478 probably due to their further oxidation to polar and oligomeric compounds, which are not
479 generally detectable using the GC–MS methods employed here. This conclusion is
480 consistent with the strong photo- and autoxidation states of palmitoleic acid (**23**) observed
481 in these samples (Fig. 4) and the differences of reactivity observed previously between
482 HBI III (**2**) and this acid in diatom cells ($k_{\text{photo HBI III}}/k_{\text{photo palmitoleic acid}} \approx 4$ and $k_{\text{auto HBI III}}/k_{\text{auto palmitoleic acid}} > 10$) (Rontani et al., 2011; 2014a).

484 In order to provide further evidence for the influence of autoxidative processes upon
485 the ratio **1/2**, we measured it, together with the autoxidation state of sitosterol (**42**)
486 (estimated on the basis of $3\beta,5\alpha,6\beta$ -trihydroxysitosterol (**43**) as previously proposed by
487 Christodoulou et al. (2009)) and palmitoleic acid (**23**) in the water column samples from
488 station 32 (T32/CTD015) and in two near-surface sediment samples from nearby locations
489 (MC45 and MC61; Fig. 1), with one of these (MC61) located directly at the station where
490 the CTD015 samples were taken. The ratio **1/2** was also measured in the surface waters
491 recovered from the top of the MC61 sediment core and in the suspension of diatomaceous
492 ‘fluff’ taken at the water-sediment interface, thereby providing a near-continuous depth
493 sequence from surface waters to underlying sediments. Although sitosterol (**42**) is
494 commonly associated with higher plants ((Lütjohann, 2004), it is also present in
495 phytoplankton, and notably in diatoms (Volkman, 1986; 2003). Due to the absence of lipid
496 signatures of terrestrial material in the water samples collected at station 32 and in the
497 sediments from nearby locations, the presence of sitosterol (**42**) in these samples was thus
498 attributed to an algal origin. The results obtained (Table 2) show a clear increase in both

499 the ratio **1/2** and the autoxidation state of algal material with water depth and then into the
500 surface sediments (Table 2). The failure to detect oxidation products of sitosterol in the
501 water column samples is attributed to the relatively poor chromatographic properties of the
502 only partially silylated (at positions 3 and 6) triol **43**, which hinders its detection at low
503 concentrations.

504 Although we do not currently have detailed taxonomic data from all sampling
505 stations/types, we do have data from the station for which we have lipid profiles from both
506 the water column and underlying Megacore (viz. CTD015 & MC61). The most striking
507 feature is the consistent decrease in the ratio (*F. curta* + *F. cylindrus*)/*F. kerguelensis*
508 through the water column, the water-sediment interface and then into the sub-surface
509 sediment (Table 2), suggesting a progressive decrease in the relative contribution of sea
510 ice-associated and open-water diatoms. However, this conclusion is contrary to what might
511 be inferred from the (increasing) IPSO₂₅ (**1**) /HBI III (**2**) ratio, suggesting that changes in
512 the latter, at some locations, are determined more by the enhanced degradation of HBI III
513 (**2**)(relative to IPSO₂₅) as shown from the lipid data described above; the caveat being that
514 the aforementioned *Fragilariopsis* spp. are not known HBI-producers. We also assume that
515 the water column data derived from samples taken in a single sampling season are also
516 representative of multi-annual accumulation that the sediment samples likely reflect.
517 Unfortunately, the known sources of IPSO₂₅ and HBI III (**2**) were of too low abundance for
518 more direct comparisons between lipid and taxonomic distributions to be made for these
519 samples. Interestingly, a positive relationship between IPSO₂₅ (**1**)/HBI III (**2**) and the ratio
520 *F. curta*/*F. kerguelensis* (i.e., a slight modification to our diatom ratio) was reported in a
521 previous downcore sediment study from the region (Massé et al., 2011), suggesting that the
522 modifications to the former described herein for the water column and water-sediment
523 interface may not necessarily have an adverse impact on its use as a proxy measure of sea

524 ice change in palaeo records, especially for qualitative purposes. Further studies comparing
525 these two approaches will, however, be required, before the generality of this observation
526 can be confirmed, and the most reliable use of IPSO₂₅/HBI III as a proxy measure of sea
527 ice change can be deciphered.

528

529 *3.2. Phytoplanktonic material from Commonwealth Bay (East Antarctica)*

530 To demonstrate the efficiency of photo- and autoxidation processes on HBI III (**2**) in
531 this region, more generally, we also analysed phytoplanktonic cells collected from surface
532 waters of Commonwealth Bay (also East Antarctica; see Fig. 1). In this weakly oxidized
533 material (oxidation percentage of palmitoleic acid (**23**) < 5%), MRM analyses allowed us
534 to detect the HBI alcohols **44–48** (Figs. 5B and 6B, Table 3). The assignment of these
535 compounds was confirmed by comparison with the MRM chromatograms of standards
536 obtained by photo- and autoxidation of HBI III (**2**) (Figs. 5A and 6A) (Rontani et al.,
537 2014b). Alcohol **48** is produced specifically by photooxidation of HBI III (**2**), while
538 alcohols **44–47** result from both its photo- and autoxidation (Rontani et al., 2014a). On the
539 basis of the detection of these oxidation products in a weakly oxidized phytoplanktonic
540 sample from Commonwealth Bay, the strong increase of the ratio IPSO₂₅ (**1**)/HBI III (**2**)
541 observed in the deeper SPM samples from stations 25, 27, 32 and 34 and in near-surface
542 sediments from the polynya region west of the Dalton Iceberg Tongue (Tables 1 and 2)
543 may be thus attributed to an intense photo- and/or autoxidation of HBI III (**2**) within the
544 water column, with further autoxidation of HBI III (**2**), relative to IPSO₂₅ (**1**), at the water-
545 sediment interface and in the oxic layer of the underlying sediment.

546 During the NaBH₄-reduction step employed to avoid thermal degradation of
547 hydroperoxides during the subsequent saponification reaction, the sum of hydroperoxides
548 and their degradation products (alcohols and ketones) was obtained via quantification of

549 their respective alcohols. Two different treatments were employed (acetylation and
550 saponification vs NaBD₄-reduction and saponification) (see Section 2.2) in order to
551 specifically quantify hydroperoxides and their main degradation products (i.e. alcohols and
552 ketones). The results obtained (summarized in Table 4) show that a substantial proportion
553 (ca. 55–81%) of HBI III (**2**) oxidation products were still present as hydroperoxides.

554 Interestingly, the decrease in unlabeled phytol (**4**) concentration (5–20%) observed
555 when the treatment of phytoplanktonic cells involved acetylation and saponification
556 instead of NaBD₄-reduction and saponification, provides further evidence for the formation
557 pathway of isophytol (**6**) proposed previously (Rontani and Galeron, 2016) (Fig. 2).
558 Indeed, this decrease likely results from the presence of 1-peroxy-3,7,11,15-
559 tetramethylhexadec-3-ene (**9**), which is formed by allylic rearrangement of its isomer **8**
560 (Fig. 2).

561

562 **4. Conclusions**

563 Selected lipids and their oxidation products were quantified in SPM samples
564 collected at different water depths in the polynya region west of the Dalton Iceberg Tongue
565 (East Antarctica). The sterol profiles were typical of mixed assemblages of diatoms,
566 prymnesiophytes and chlorophytes. Surprisingly, some samples contained
567 depolymerisation products of cutins, the presence of which was attributed to the
568 accumulation of low-density debris of the two phanerogams present in Antarctica.

569 We identified an intense photo- and autoxidation of unsaturated diatom components
570 (e.g. palmitoleic acid (**23**), 24-methylenecholesterol (**13**), chlorophyll phytyl side-chain
571 (**4**)), but not of HBI III (**2**), despite its known reactivity towards such processes, likely due
572 to its susceptibility towards further oxidation. However, oxidation products of HBI III (**2**)

573 could be detected in weakly oxidized SPM samples collected from Commonwealth Bay
574 (East Antarctica), clearly demonstrating the oxidation of this lipid in this region.

575 The systematic increase of the ratio IPSO₂₅ (1)/HBI III (2) observed with depth in the
576 water column and in some underlying sediments thus appears to result, in part, from an
577 intense and preferential abiotic degradation of the HBI III (2) due to a combination of
578 photo- and autoxidation processes (Fig. 7). At one sampling site, the increase in the IPSO₂₅
579 (1)/HBI III (2) ratio with depth was opposite to that of the ratio of selected sea ice-
580 associated versus open-water diatoms, suggesting that the differential biomarker
581 degradation was a dominant factor. However, for another sampling site, the increase in the
582 IPSO₂₅ (1)/HBI III (2) ratio appeared to be more influenced by the accumulation of ice
583 algal material, although we do not yet have the complementary taxonomic data to confirm
584 this.

585 Distinguishing between these two factors will require more detailed and combined
586 lipid and taxonomic analysis in the future. In the meantime, it is evident from the results
587 presented here, that the differential degradation of IPSO₂₅ (1) and HBI III (2) in the water
588 column and in near-surface sediments (at least) can impact on the ratio between these two
589 HBIs between their source and sedimentary environments. The latter should be taken into
590 account when using this parameter for palaeo sea ice reconstruction purposes in the
591 Antarctic. The extent to which the IPSO₂₅ (1)/HBI III (2) ratio reflects established proxy
592 measures of past sea ice change (e.g., the ratio of certain *Fragilariopsis* spp. as described
593 herein) will require more studies of both parameters in further downcore records from the
594 Antarctic.

595

596 **Acknowledgements**

597

598 The FEDER OCEANOMED (N° 1166-39417) is acknowledged for the funding of the
599 apparatus employed. Thanks are due to the scientific party and crew of cruise NBP1402;
600 the project (P.I. A. Leventer) was funded by NSF ANT-1143836. We also thank G. Massé
601 for the donation of the phytoplankton samples collected in the Commonwealth Bay during
602 the IPEV-COCA2012 cruise funded by IPEV (1010-ICELIPIDS program) and ANR
603 (CLIMICE program). We thank two anonymous referees for their useful and constructive
604 comments.

605

606 **References**

607

- 608 Alldredge, A.L., Passow, U., Logan, B.E., 1993. The abundance and significance of a class
609 of large, transparent organic particles in the ocean. *Deep-Sea Research Part I-*
610 *Oceanographic Research Papers* 40, 1131-1140.
- 611 Armand, L., Crosta, X., Romero, O., Pichon, J.J., 2005. The biogeography of major diatom
612 taxa in Southern Ocean sediments.1. Sea ice related species. *Palaeogeography,*
613 *Palaeoclimatology, Palaeoecology* 223, 93–126.
- 614 Armand, L.K., Ferry, A., Leventer, A., 2017. Advances in palaeo sea ice estimation. In:
615 Thomas, D.N. (Ed.), *Sea Ice*. John Wiley & Sons Ltd, Chichester, pp. 600–629.
- 616 Barbara, L., Crosta, X., Massé, G., Ther, O., 2010. Deglacial environments in eastern
617 Prydz Bay, East Antarctica. *Quaternary Science Reviews* 29, 2731–2740.
- 618 Barbara, L., Crosta, X., Schmidt, S., Massé, G., 2013. Diatoms and biomarkers evidence
619 for major changes in sea ice conditions prior the instrumental period in Antarctic
620 Peninsula. *Quaternary Science Reviews* 79, 99–110.

621 Barbara, L., Crosta, X., Leventer, A., Schmidt, S., Etourneau, J., Domack, E., Massé, G.,
622 2016. Environmental responses of the Northeast Antarctic Peninsula to the Holocene
623 climate variability, *Paleoceanography*, 31, 131–147.

624 Belt, S.T., Cooke, D.A., Robert, J.-M., Rowland, S.J., 1996. Structural characterisation of
625 widespread polyunsaturated isoprenoid biomarkers: A C₂₅ triene, tetraene and pentaene
626 from the diatom *Haslea ostrearia* Simonsen. *Tetrahedron Letters* 37, 4755–4758.

627 Belt, S.T., Allard, W.G., Massé, G., Robert, J.-M., Rowland, S.J., 2000. Highly branched
628 isoprenoids (HBIs): identification of the most common and abundant sedimentary
629 isomers. *Geochimica et Cosmochimica Acta* 64, 3839–3851.

630 Belt, S.T., Massé, G., Rowland, S.J., Poulin, M., Michel, C., LeBlanc, B., 2007. A novel
631 chemical fossil of palaeo sea ice: IP₂₅. *Organic Geochemistry* 38, 16–27.

632 Belt, S.T., Müller, J., 2013. The Arctic sea ice biomarker IP₂₅: a review of current
633 understanding, recommendations for future research and applications in palaeo sea ice
634 reconstructions. *Quaternary Science Reviews* 79, 9–25.

635 Belt, S.T., Brown, T.A., Ampel, L., Cabedo-Sanz, P., Fahl, K., Kocis, J.J., Masse, G.,
636 Navarro-Rodriguez, A., Ruan, J., Xu, Y., 2014. An inter-laboratory investigation of
637 the Arctic sea ice biomarker proxy IP₂₅ in marine sediments: key outcomes and
638 recommendations. *Climate of the Past* 10, 155–166.

639 Belt, S.T., Cabedo-Sanz, P., Smik, L., Navarro-Rodriguez, A., Berben, S.M.P., Knies, J.,
640 Husum, K., 2015. Identification of paleo Arctic winter sea ice limits and the marginal
641 ice zone: Optimised biomarker-based reconstructions of late Quaternary Arctic sea ice.
642 *Earth and Planetary Science Letters* 431, 127–139.

643 Belt, S.T., Smik, L., Brown, T.A., Kim, J.H., Rowland, S.J., Allen, C.S., Gal, J.K., Shin,
644 K.H., Lee, J.I., Taylor, K.W.R., 2016. Source identification and distribution reveals

645 the potential of the geochemical Antarctic sea ice proxy IPSO₂₅. Nature
646 Communications 7, 12655.

647 Belt, S.T., Brown, T.A., Smik, L., Assmy, P., Mundy, C.J., 2018. Sterol identification in
648 floating Arctic sea ice algal aggregates and the Antarctic sea ice diatom *Berkeleya*
649 *adeliensis*. Organic Geochemistry 118, 1–3.

650 Belt, S.T., 2018. Source-specific biomarkers as proxies for Arctic and Antarctic sea ice.
651 Organic Geochemistry 125, 273-295.

652 Berkessel, A., 2014. Science of Synthesis: Houben-Weyl Methods of Molecular
653 Transformations, Vol. 38: Peroxides, Georg Thieme Verlag, p. 75.

654 Brown, T.A., Belt, S.T., Tatarek, A., Mundy, C.J., 2014c. Source identification of the
655 Arctic sea ice proxy IP₂₅. Nature Communications 5, 4197.

656 Campagne, P., Costa, X., Houssais, M.N., Swingedouw, D., Schmidt, S., Martin, A.,
657 Devred, E., Capo, S., Marieu, V., Closset, I., Massé, G., 2015 Glacial ice and
658 atmospheric forcing on the Mertz Glacier Polynya over the past 250 years. Nature
659 Communications 6, 6642.

660 Campagne, P., Crosta, X., Schmidt, S., Houssais, M.N., Ther, O., Massé, G., 2016.
661 Sedimentary response to sea ice and atmospheric variability over the instrumental
662 period off Adélie Land, East Antarctica. Biogeosciences 13, 4205–4218.

663 Christodoulou S., Marty J.-C., Miquel J.-C., Volkman J.K., Rontani J.-F., 2009. Use of
664 lipids and their degradation products as biomarkers for carbon cycling in the
665 northwestern Mediterranean Sea. Marine Chemistry 113, 25-40.

666 Collins, L.G., Allen, C.S., Pike, J., Hodgson, D.A., Weckström, K., Massé, G., 2013.
667 Evaluating highly branched isoprenoid (HBI) biomarkers as a novel Antarctic sea-ice
668 proxy in deep ocean glacial age sediments. Quaternary Science Reviews 79, 87–98.

669 Crosta, X., Koc, N., 2007. Diatoms: From micropaleontology to isotope geochemistry, in:
670 Methods in Late Cenozoic Paleoceanography, Hilaire-Marcel, C. and de Vernal, A.
671 (Eds.), Elsevier, Amsterdam, the Netherlands, pp. 327–369.

672 Crosta, X., Romero, O., Armand, L., Pichon, J.J., 2005. The biogeography of major diatom
673 taxa in Southern Ocean sediments. 2. Open Ocean related species. *Palaeogeography,*
674 *Palaeoclimatology, Palaeoecology* 223, 66–92.

675 Crosta, X., Denis, D., Ther, O., 2008. Sea ice seasonality during the Holocene, Adelie
676 Land, East Antarctica. *Marine Micropaleontology* 66, 222–232.

677 Cuny, P., Rontani, J.-F., 1999. On the widespread occurrence of 3-methylidene-7,11,15-
678 trimethylhexadecan-1,2-diol in the marine environment: a specific isoprenoid marker
679 of chlorophyll photodegradation. *Marine Chemistry* 65, 155-165.

680 Cuny, P., Marty, J.-C., Chiaverini, J., Vescovali, I., Raphel, D., Rontani, J.-F., 2002. One-
681 year seasonal survey of the chlorophyll photodegradation process in the Northwestern
682 Mediterranean Sea. *Deep-Sea Research II* 49, 1987-2005.

683 Deas, A.H.B., Holloway, P.J., 1977. The intermolecular structure of some plant cutins. In:
684 Tevini, M., Lichtenthaler, H. (Eds.), *Lipids and Lipid Polymers in Higher Plants.*
685 Springer, Berlin, pp. 293-299.

686 Denis, D., Crosta, X., Barbara, L., Massé, G., Renssen, H., Ther, O., Giraudeau, J., 2010.
687 Sea ice and wind variability during the Holocene in East Antarctica: insight on
688 middle-high latitude coupling. *Quaternary Science Reviews* 29, 3709–3719.

689 de Leeuw, J.W., Correia, V.A., Schenck, P.A., 1974. On the decomposition of phytol under
690 simulated geological conditions and in the top-layer of natural sediments. In: Tissot,
691 B., Bierner, F. (Eds.), *Advances in Organic Geochemistry 1973.* Editions Technip,
692 Paris, pp. 993–1004.

693 de Leeuw, J.W., Baas, M., 1986. Early-stage diagenesis of steroids. In: Johns, R.B. (Ed.),
694 Biological Markers in the Sedimentary Record. Elsevier, Amsterdam, pp. 101-123.

695 de Vernal, A., Gersonde, R., Goosse, H., Seidenkrantz, M.-S., Wolff, E.W., 2013. Sea ice
696 in the paleoclimate system: the challenge of reconstructing sea ice from proxies – an
697 introduction. *Quaternary Science Reviews* 79, 1–8.

698 Dickson, R., Rudels, B., Dye, S., Karcher, M., Meincke, J., Yashayaev, I., 2007. Current
699 estimates of freshwater flux through Arctic and subarctic seas. *Progress in*
700 *Oceanography* 73, 210–230.

701 Etourneau, J., Collins, L.G., Willmott, V., Kim, J.H., Barbara, L., Leventer, A., Schouten,
702 S., Sinninghe Damsté, J.S., Bianchini, A., Klein, V., Crosta, X., Massé, G., 2013.
703 Holocene climate variations in the western Antarctic Peninsula: evidence for sea ice
704 extent predominantly controlled by changes in insolation and ENSO variability.
705 *Climate of the Past* 9, 1431–1446.

706 Fahl, K., Kattner, G., 1993. Lipid content and fatty acid composition of algal communities
707 in sea-ice and water from Weddell Sea (Antarctica). *Polar Biology* 13, 405-409.

708 Fang, J., Chan, O., Joeckel, R.M., Huang, Y., Wang, Y., Bazyliniski, D.A., Moorman, T.B.,
709 Ang Clement, B.J., 2006. Biomarker analysis of microbial diversity in sediments of a
710 saline groundwater seep of Salt Basin, Nebraska. *Organic Geochemistry* 37, 912-931.

711 Fetterer F., Knowles K., Meier W.N., Savoie M., 2016. Sea Ice Index. ver.2 NSIDC:
712 National Snow and Ice Data Center. Boulder, Colorado
713 (<https://doi.org/10.7265/N5736NV7>) [Digital Media, updated daily].

714 IPCC, 2013: Summary for Policymakers. In: *Climate Change 2013: The Physical*
715 *Science Basis. Contribution of Working Group I to the Fifth Assessment Report of the*
716 *Intergovernmental Panel on Climate Change* [Stocker, T.F., D. Qin, G.-K. Plattner, M.

717 Tignor, S.K. Allen, J. Boschung, A. Nauels, Y. Xia, V. Bex and P.M. Midgley (eds.)].
718 Cambridge University Press, Cambridge, United Kingdom and New York, NY, USA.
719 Frankel, E.N., 1998. Lipid Oxidation. The Oily Press, Dundee.
720 Frimer, A.A., 1979. The reaction of singlet oxygen with olefins: the question of
721 mechanism. Chemical Review 79, 359-387.
722 Gagosian, R.B., Smith, S.O., Nigrelli, G.E., 1982. Vertical transport of steroid alcohols and
723 ketones measured in a sediment trap experiment in the equatorial Atlantic Ocean.
724 Geochimica et Cosmochimica Acta 46, 1163-1172.
725 Hasle, G.R., 1965. *Nitzschia* and *Fragilariopsis* species studied in the light and electron
726 microscopes III. The genus *Fragilariopsis*. Skr. Norske Vidensk-Akad. I. Mat.-Nat.
727 Kl. Ny Serie 21, 1-49.
728 Holland, H.L., Diakow, P.R.P., 1979. Microbial hydroxylation of steroids. 5. Metabolism
729 of androst-5-en-3,17-dione and related compounds by *Rhizopus arrhizus* ATCC
730 11145. Canadian Journal of Chemistry 57, 436-440.
731 Johns, L., Wraige, E.J., Belt, S.T., Lewis, C.A., Massé, G., Robert, J.M., Rowland, S.J.,
732 1999. Identification of a C₂₅ highly branched isoprenoid (HBI) diene in Antarctic
733 sediments, Antarctic sea-ice diatoms and cultured diatoms. Organic Geochemistry 30,
734 1471-1475.
735 Kattner, G., Cercken, G., Eberlein, K., 1983. Development of lipid during a spring bloom
736 in the northern North Sea. I. Particulate fatty acids. Marine Chemistry 14, 149-162.
737 Kim, S.Y., Choi, J.K., Dolan, J.R., Shin, H.C., Lee, S., Yang, E.J., 2013. Morphological
738 and ribosomal DNA-based characterization of six Antarctic ciliate morphospecies
739 from the Amundsen Sea with phylogenetic analyses. Journal of Eukaryotic
740 Microbiology 60, 497-513.

741 Kolattukudy, P.E., 1977. Lipid polymers and associated phenols, their chemistry,
742 biosynthesis, and role in pathogenesis, *Recent Advances in Phytochemistry* 77, 185-
743 246.

744 Kolattukudy, P.E., 1980. Cutin, suberin and waxes. In: Stumpf, P.K., Conn, E.E. (Eds.),
745 *The Biochemistry of Plants*, vol. 4. Academic Press, Davis, pp. 571–645.

746 Lee, C., Gagosian, R.B., Farrington, J.W., 1980. Geochemistry of sterols in sediments from
747 Black Sea and the southwest African shelf and slope, *Organic Geochemistry* 2, 103-
748 113.

749 Leventer, A., 2013. The fate of Antarctic “sea ice diatoms” and their use as
750 paleoenvironmental indicators. In: Lizotte, M.P., Arrigo, K.R. (Eds.), *Antarctic Sea*
751 *Ice: Biological processes, Interactions and Variability*. American Geophysical Union,
752 pp. 121–137.

753 Leventer, A., Armand, L., Harwood, D.M., Jordan, R., Ligowski, R., 2008. New
754 approaches and progress in the use of polar marine diatoms in reconstructing sea ice
755 distribution. *Papers in the Earth and Atmospheric Sciences*. Paper 287.

756 Leventer, A., 1998. The fate of sea ice diatoms and their use as paleoenvironmental
757 indicators. In: Lizotte, M.P. and Arrigo, K.R. (Eds.), *Antarctic Sea Ice: Biological*
758 *Processes*, AGU Research Series 73, Washington, D.C., pp. 121–137.

759 Leu, E., Wiktor, J., Soreide, J.E., Berge, J., Falk-Petersen, S., 2010. Increased irradiance
760 reduces food quality of sea ice algae. *Marine Ecology Progress Series* 411, 49-60.

761 Loidl-Stahlhofen, A., Spiteller, G., 1994. α -Hydroxyaldehydes, products of lipid
762 peroxidation. *Biochimica et Biophysica Acta* 1211, 156-160.

763 Lütjohann, D., 2004. Sterol autoxidation: from phytosterols to oxyphytosterols. *British*
764 *Journal of Nutrition* 91, 3-4.

765 Marchand, D., Rontani, J.-F., 2001. Characterisation of photooxidation and autoxidation
766 products of phytoplanktonic monounsaturated fatty acids in marine particulate matter
767 and recent sediments. *Organic Geochemistry* 32, 287-304.

768 Marchand, D., Rontani, J.-F., 2003. Visible light-induced oxidation of lipid components of
769 purple sulfur bacteria: a significant process in microbial mats. *Organic Geochemistry*
770 34, 61-79.

771 Martin-Creuzburg, D., Beck, B., Freese, H.M., 2011. Food quality of heterotrophic bacteria
772 for *Daphnia magna*: evidence for a limitation by sterols. *FEMS Microbiology* 76,
773 592-601.

774 Martin-Creuzburg, D., Merkel, P., 2016. Sterols of freshwater microalgae: potential
775 implications for zooplankton nutrition. *Journal of Plankton Research* 38, 865-877.

776 Mihara, S., Tateba, H., 1986. Photosensitized oxygenation reactions of phytol and its
777 derivatives. *The Journal of Organic Chemistry* 51, 1142-1144.

778 Passow, U., 2002. Transparent exopolymer particles (TEP) in aquatic environments.
779 *Progress in Oceanography* 55, 287-333.

780 Pedersen, L., Jensen, H.M., Burmeister, A.D., Hansen, B.W., 1999. The significance of
781 food web structure for the condition and tracer lipid content of juvenile snail fish
782 (*Pisces*: *Liparis* spp.) along 65–728N off West Greenland. *Journal of Plankton*
783 *Research* 21, 1593-1611.

784 Perette, M., Yool, A., Quartly, G.D., Popova, E.E., 2011. Near-ubiquity of ice-edge blooms in
785 the Arctic. *Biogeosciences* 8, 515–524.

786 Porter, N.A., Caldwell, S.E., Mills, K.A., 1995. Mechanisms of free radical oxidation of
787 unsaturated lipids. *Lipids* 30, 277-290.

788 Prahl, F.G., Eglinton, G., Corner, E.D.S., O'Hara, S.C.M., Forsberg, T.E.V., 1984. Changes
789 in plant lipids during passage through the gut of *Calanus*. Journal of the Marine
790 Biological Association of the United Kingdom 64, 317-334.

791 Reuss, N., Poulsen, L.K., 2002. Evaluation of fatty acids as biomarkers for a natural plankton
792 community. A field study of a spring bloom and a post-bloom period off West
793 Greenland. Marine Biology 141, 423-434.

794 Riebesell U., Schloss I., Smetacek V., 1991. Aggregation of algae released from melting sea
795 ice-implications for seeding and sedimentation. Polar Biology 11,239-248.

796 Rampen, S.W., Abbas, B.A., Schouten, S., Sinninghe Damsté, J.S., 2010. A comprehensive
797 study of sterols in marine diatoms (Bacillariophyta): implications for their use as tracers
798 for diatom productivity. Limnology and Oceanography 55, 91–105.

799 Rontani, J.-F., Grossi, V., Faure, F., Aubert, C., 1994. “Bound” 3-methylidene-7,11,15-
800 trimethylhexadecan-1,2-diol: a new isoprenoid marker for the photodegradation of
801 chlorophyll-a in seawater. Organic Geochemistry 21, 135-142.

802 Rontani, J.-F., Cuny, P., Grossi, V., 1998. Identification of a pool of lipid photoproducts in
803 senescent phytoplanktonic cells. Organic Geochemistry 29, 1215-1225.

804 Rontani, J.-F., Bonin, P., Volkman, J.K., 1999. Biodegradation of free phytol by bacterial
805 communities isolated from marine sediments under aerobic and denitrifying conditions.
806 Applied and Environmental Microbiology 65, 5484–5492.

807 Rontani, J.-F., Volkman, J.K., 2003. Phytol degradation products as biogeochemical tracers in
808 aquatic environments. Organic Geochemistry 34, 1-35.

809 Rontani, J.-F., Aubert, C., 2005. Characterization of isomeric allylic diols resulting from
810 chlorophyll phytol side chain photo- and autoxidation by electron ionization gas
811 chromatography/mass spectrometry. Rapid Communications in Mass Spectrometry 19,
812 637-646.

813 Rontani, J.-F., Zabeti, N., Wakeham, S.G., 2009. The fate of marine lipids: Biotic vs. abiotic
814 degradation of particulate sterols and alkenones in the Northwestern Mediterranean Sea.
815 *Marine Chemistry* 113, 9-18.

816 Rontani, J.-F., Belt, S.T., Vaultier, F., Brown, T.A., 2011. Visible light-induced photo-
817 oxidation of highly branched isoprenoid (HBI) alkenes: a significant dependence on the
818 number and nature of the double bonds. *Organic Geochemistry* 42, 812-822.

819 Rontani, J.-F., 2012. Photo- and free radical-mediated oxidation of lipid components
820 during the senescence of phototrophic organisms. In: T. Nagata Ed., *Senescence*.
821 Intech, Rijeka, pp. 3-31.

822 Rontani, J.-F., Charriere, B., Forest, A., Heussner, S., Vaultier, F., Petit, M., Delsaut, N.,
823 Fortier, L., Sempéré, R., 2012. Intense photooxidative degradation of planktonic and
824 bacterial lipids in sinking particles collected with sediment traps across the Canadian
825 Beaufort Shelf (Arctic Ocean). *Biogeosciences* 9, 4787-4802.

826 Rontani, J.-F., Charrière, B., Sempéré, R., Doxaran, D., Vaultier, F., Vonk, J.E., Volkman,
827 J.K., 2014a. Degradation of sterols and terrigenous organic matter in waters of the
828 Mackenzie Shelf, Canadian Arctic. *Organic Geochemistry* 75, 61-73.

829 Rontani, J.-F., Belt, S., Vaultier, F., Brown, T., Massé, G., 2014b. Autoxidative and
830 photooxidative reactivity of highly branched isoprenoid (HBI) alkenes. *Lipids*, 49(5),
831 481-494.

832 Rontani, J.-F., Galeron, M.-A., 2016. Autoxidation of chlorophyll phytyl side-chain in
833 senescent phototrophic organisms: a potential source of isophytol in the environment.
834 *Organic Geochemistry* 97, 37-40.

835 Rontani, J.-F., Amiraux, R., Lalande, C., Babin, M., Kim, H.-R., Belt, S.T., 2018. Use of
836 palmitoleic acid and its oxidation products for monitoring the degradation of ice algae
837 in Arctic waters and bottom sediments. *Organic Geochemistry* 124, 88-102.

838 Rossi, S., Sabates, A., Latasa, M., reyes, E., 2006. Lipid biomarkers and trophic linkages
839 between phytoplankton, zooplankton and anchovy (*Engraulis encrasicolus*) larvae in
840 the NW Mediterranean. *Journal of Plankton Research* 28, 551-562.

841 Sakshaug, E., Johnsen, G., Kristiansen, S., von Quillfeldt, C., Rey, F., Slagstad, D.,
842 Thingstad, F., 2009. Phytoplankton and primary production. In: Sakshaug, E.,
843 Johnsen, G., Kovacs, K. (Eds), *Ecosystem Barents Sea*. Tapir Academic Press,
844 Trondheim, pp.167–208.

845 Scherer, R.P., 1994. A new method for the determination of absolute abundance of diatoms
846 and other silt-sized sedimentary particles. *Journal of Paleolimnology* 12 (1), 171–178.

847 Schmidt, K., Brown, T.A., Belt, S.T., Ireland, L.C., Taylor, K.W.R., Thorpe, S.E., Ward,
848 P., Atkinson, A., 2018. Do pelagic grazers benefit from sea ice? Insights from the
849 Antarctic sea ice proxy IPSO₂₅. *Biogeosciences* 15, 1987– 2006.

850 Schrader, H.J., Gersonde, R., 1978. Diatoms and silicoflagellates. In: Zachariasse, A. (Ed.),
851 *Micropaleontological Counting Methods and Techniques - An Exercise on Eight*
852 *Meters Section of the Lower Pliocene of Capo Rossello, Sicily*. Utrecht
853 *Micropaleontology Bulletin*, 17, pp. 129–176.

854 Scott, F., Marchant, H.J., 2005. *Antarctic Marine Protists* 1st ed. F. Scott and H. J.
855 Marchant, eds., Canberra, Hobart: Australian Biological Resources Study and
856 Australian Antarctic Division.

857 Serreze, M.C., Stroeve, J., Barrett, A.P., Boisvert, L.N., 2016. Summer atmospheric
858 circulation anomalies over the Arctic Ocean and their influence on September sea ice
859 extent. A cautionary tale. *Journal of Geophysical Research: Atmospheres* 121, 11463–
860 11485.

861 Smik, L., Belt, S.T., Lieser, J.L., Armand, L.K., Leventer, A., 2016. Distributions of highly
862 branched isoprenoid alkenes and other algal lipids in surface waters from East

863 Antarctica: Further insights for biomarker-based paleo sea-ice reconstruction. *Organic*
864 *Geochemistry* 95, 71–80.

865 Smith, L.L., 1981. The autoxidation of cholesterol. Plenum Press, New York, pp. 119-132.

866 Smith, R.I.L., 1994. Vascular plants as bioindicators of regional warming in Antarctica.
867 *Oecologia* 99, 322-328.

868 Smith, W.O., 1987. Phytoplankton dynamics in marginal ice zones. *Oceanography and*
869 *Marine Biology* 25, 11–38.

870 Smith, W.O., Jr., Nelson, D.M., 1986. The importance of ice-edge blooms in the Southern
871 Ocean. *Biosciences* 36, 251–257.

872 Stroeve, J.C., Serreze, M.C., Holland, M.M., Kay, J.E., Malanik, J., Barrett, A.P., 2012.
873 The Arctic’s rapidly shrinking sea ice cover: a research synthesis. *Climate Change*
874 110, 1005–1027.

875 Thomas, D.N., 2017. *Sea ice* 3rd ed. Wiley-Blackwell: pp 664.

876 Tomas, C.R., 1997. *Identifying marine phytoplankton*, San Diego: Academic Press.

877 Utermöhl, H., 1958. Zur Vervollkommnung der quantitativen Phytoplankton-Methodik.
878 *Internationale Vereinigung für theoretische und angewandte Limnologie: Mitteilungen*
879 9, 1–38.

880 Volkman, J.K., Corner, E.D.S., Eglinton, G., 1980. Transformations of biolipids in the
881 marine food web and in underlying bottom sediments, *Colloque International du*
882 *Centre National de la Recherche Scientifique* 293, 185-197.

883 Volkman, J.K., 1986. A review of sterol markers for marine and terrigenous organic
884 matter. *Organic Geochemistry* 9, 83-99.

885 Volkman, J.K., 2003. Sterols in microorganisms. *Applied Microbiology and*
886 *Biotechnology* 60, 495-506.

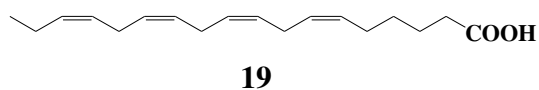
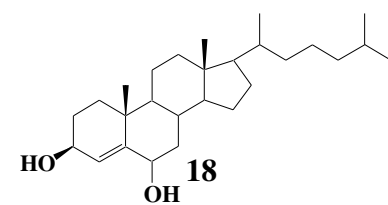
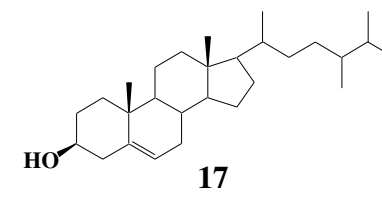
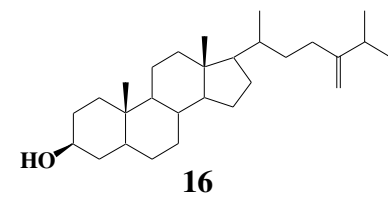
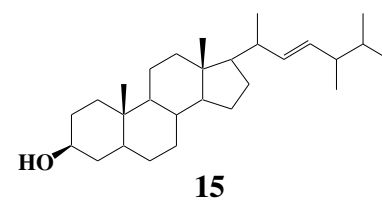
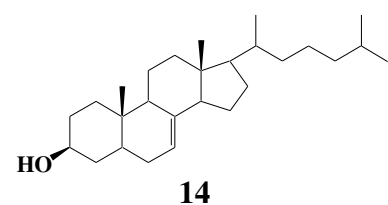
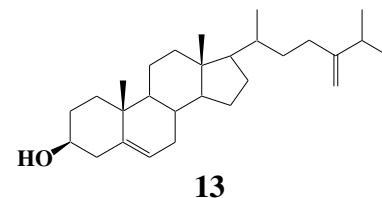
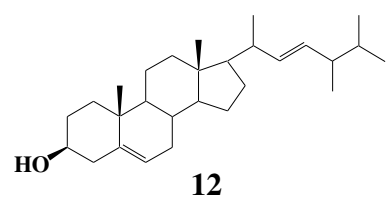
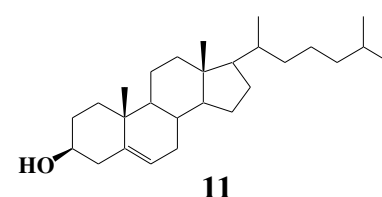
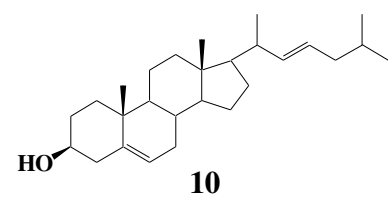
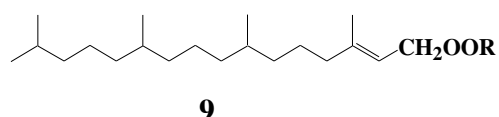
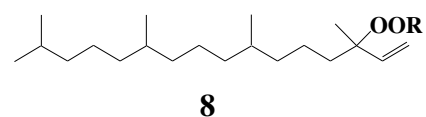
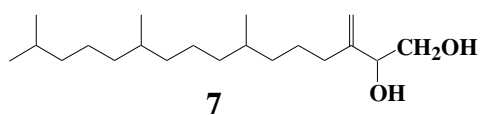
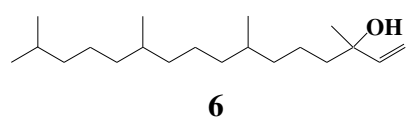
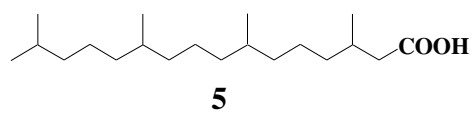
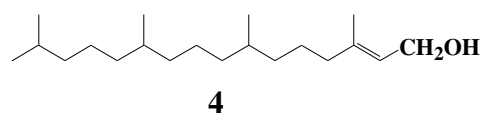
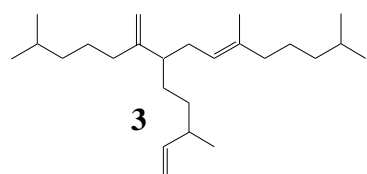
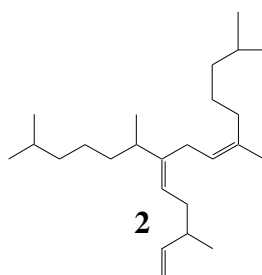
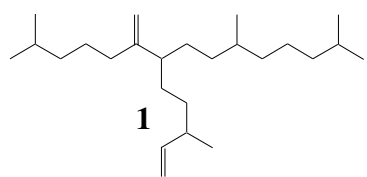
887 Walsh, J.E., Fetterer, F., Scott Stewart, J., Chapman, W.L., 2017. A database for depicting
888 Arctic sea ice variations back to 1850. *Geographical Review* 107, 89–107.

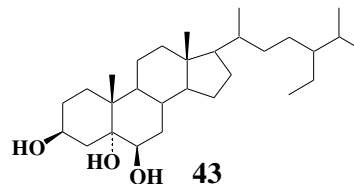
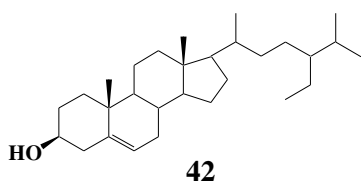
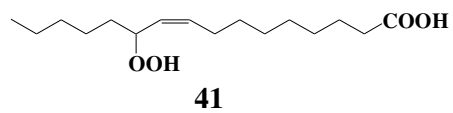
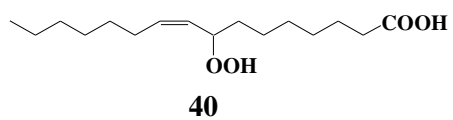
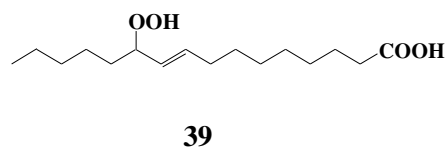
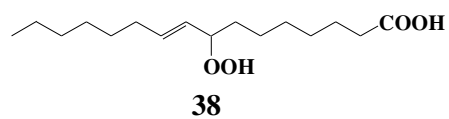
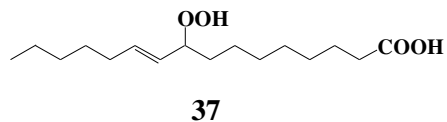
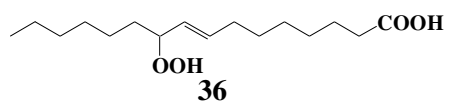
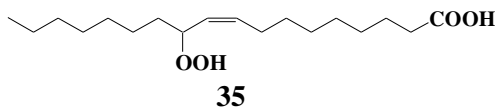
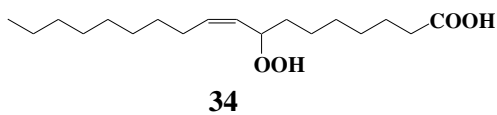
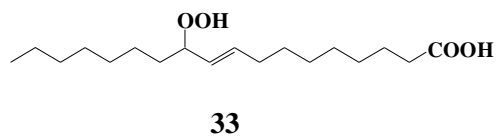
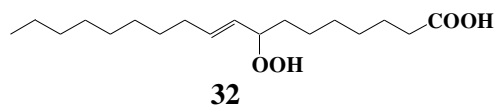
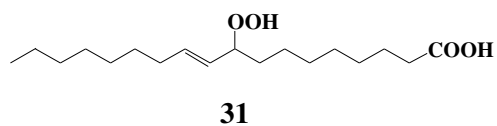
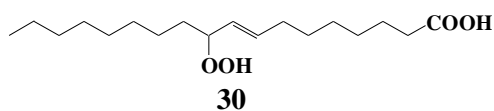
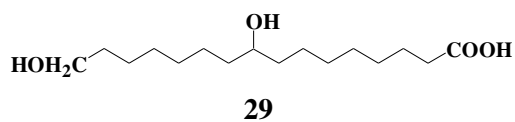
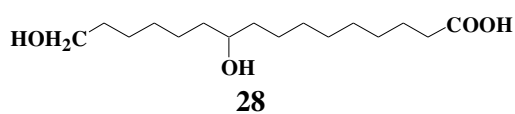
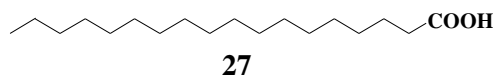
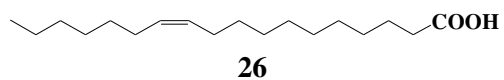
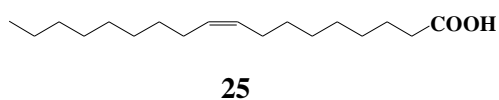
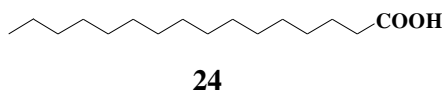
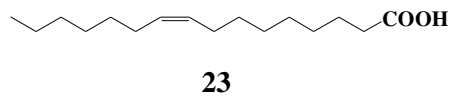
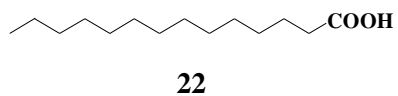
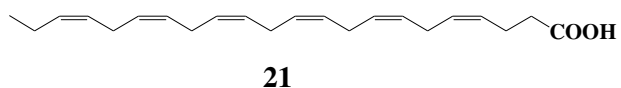
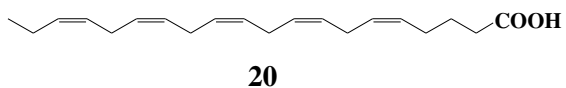
889 Wakeham, S.G., 1989. Reduction of stenols to stanols in particulate matter at oxic-anoxic
890 boundaries in seawater. *Nature* 342, 787-790.

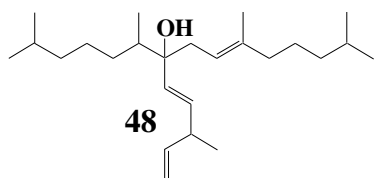
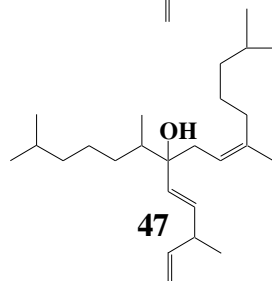
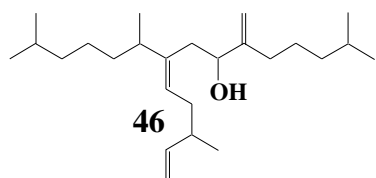
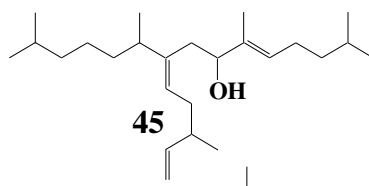
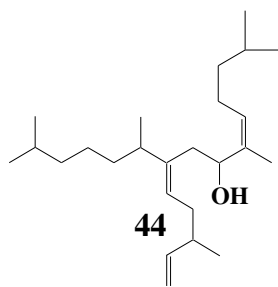
891 Yin, H., Xu, L., Porter, N.A., 2011. Free radical lipid peroxidation: mechanisms and
892 analysis. *Chemical Review* 111, 5944-5972.

893

APPENDIX







896

897 **FIGURE CAPTIONS**

898

899 Figure 1. Summary map showing sampling locations (CB = Commonwealth Bay).

900

901 Figure 2. Proposed pathways for autoxidation of chlorophyll phytyl side chain.

902

903 Figure 3. Photooxidation percentages of *epi*-brassicasterol (**12**), 24-methylenecholesterol
904 (**13**) and chlorophyll in the CTD samples collected at the stations selected for lipid
905 oxidation product analyses. The very low photooxidation percentages of sterols in the
906 samples collected at the station 32 were not included in this figure.

907

908 Figure 4. Photo- and autoxidation percentages of palmitoleic (**23**) and oleic (**25**) acids in
909 the CTD samples collected at the stations selected for lipid oxidation product analyses. The
910 weak oxidation percentages of palmitoleic acid in the samples collected at the station 32
911 are given in Table 3.

912

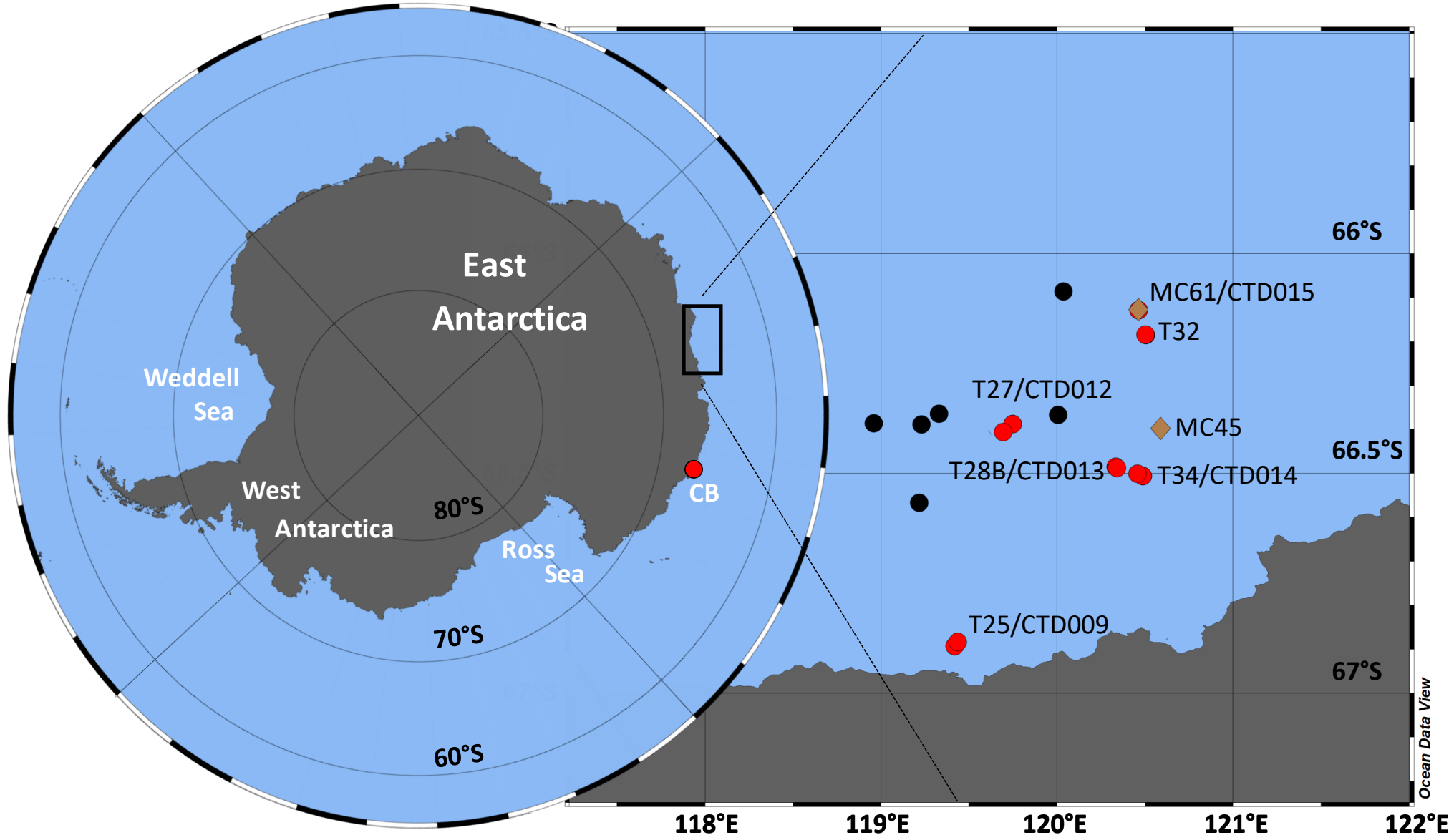
913 Figure 5. MRM chromatograms (m/z 213 \rightarrow 117, m/z 213 \rightarrow 123 and m/z 213 \rightarrow 157) for
914 standard oxidation products of HBI III (**2**) (A) and CB phytoplanktonic sample collected in
915 Commonwealth Bay (B).

916

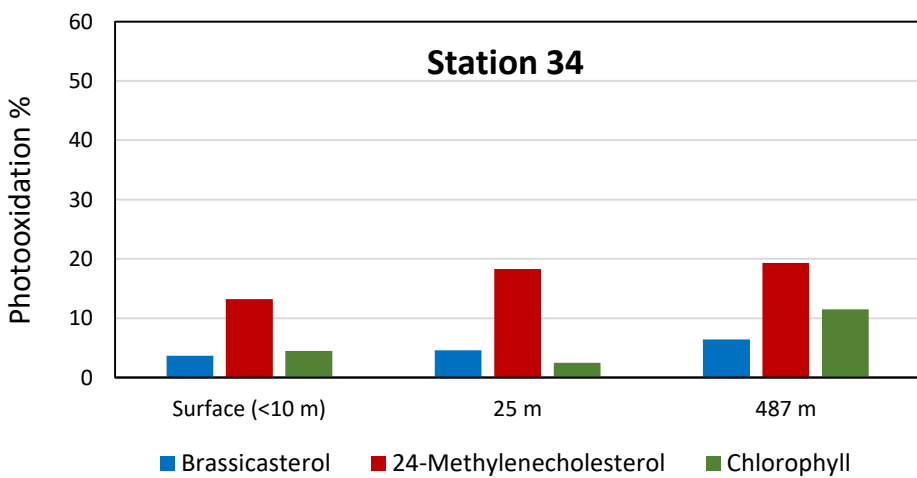
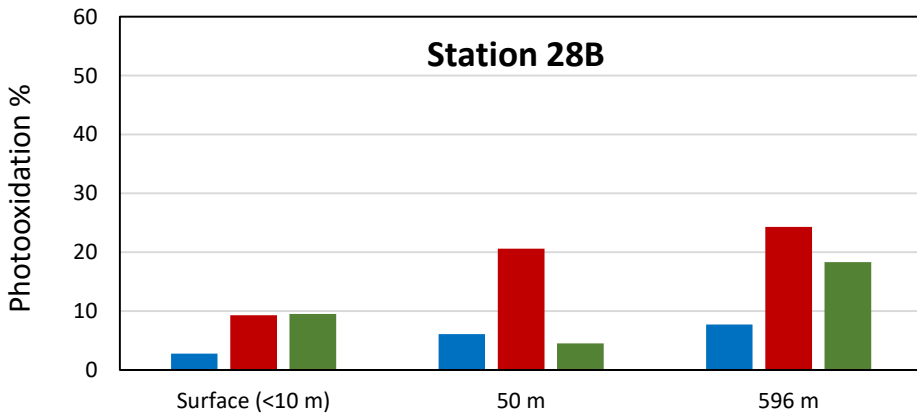
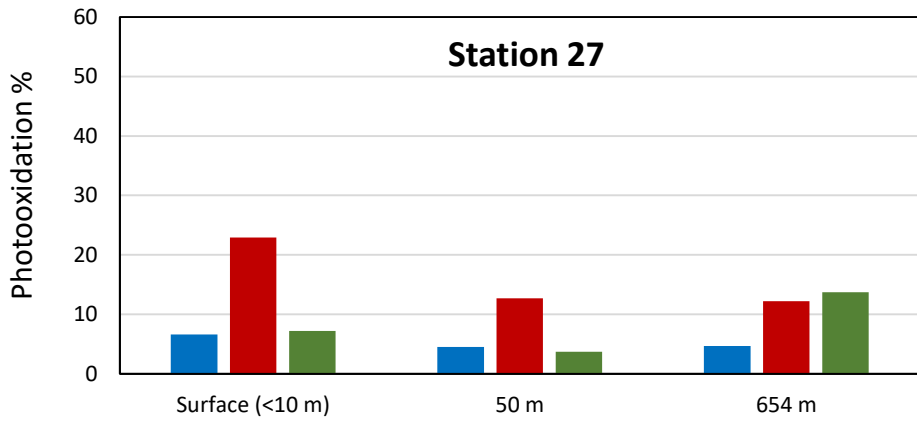
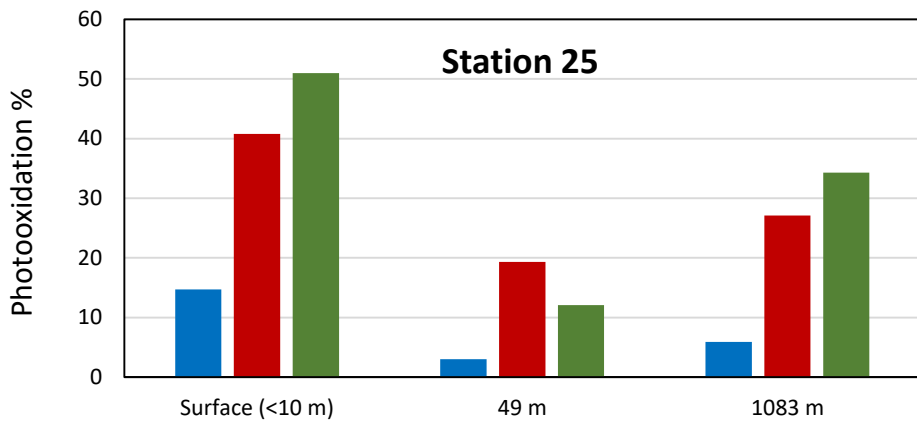
917 Figure 6. MRM chromatograms (m/z 295 \rightarrow 93, m/z 295 \rightarrow 107 and m/z 295 \rightarrow 183) for
918 standard oxidation products of the HBI III (2) (A) and CB phytoplanktonic sample
919 collected from Commonwealth Bay (B).

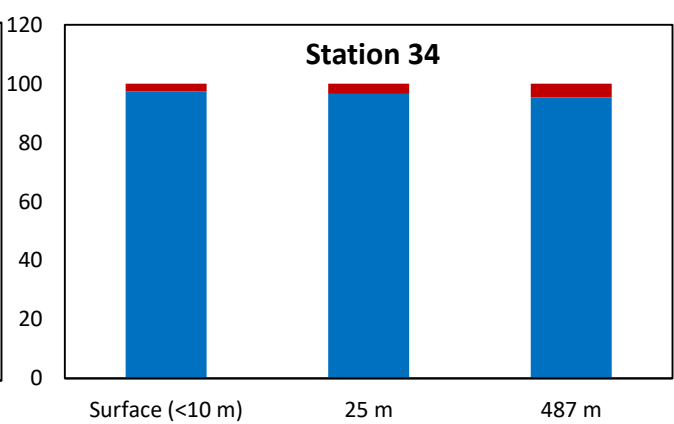
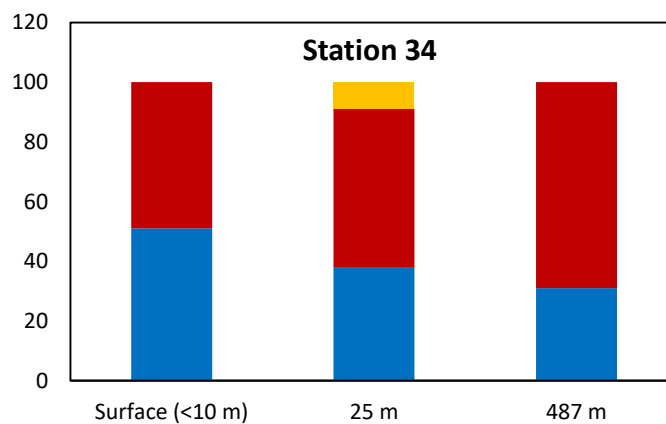
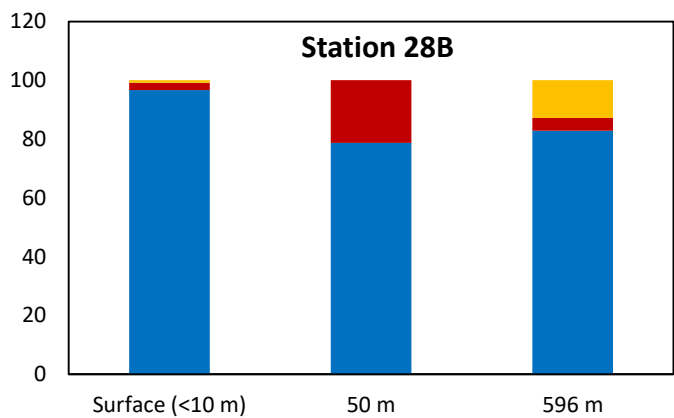
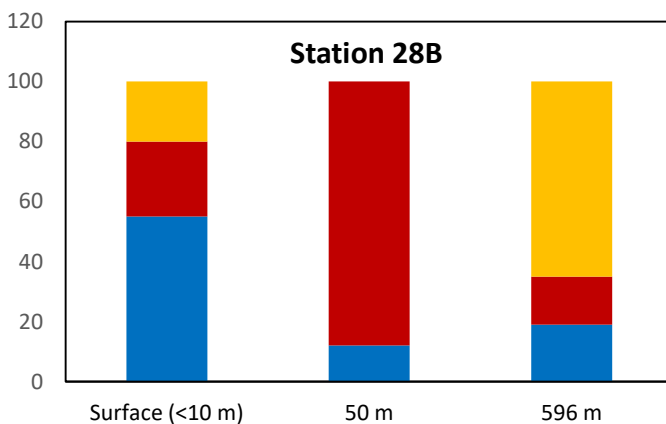
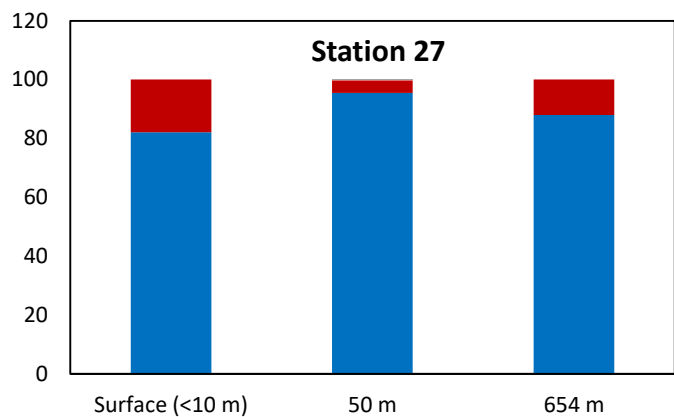
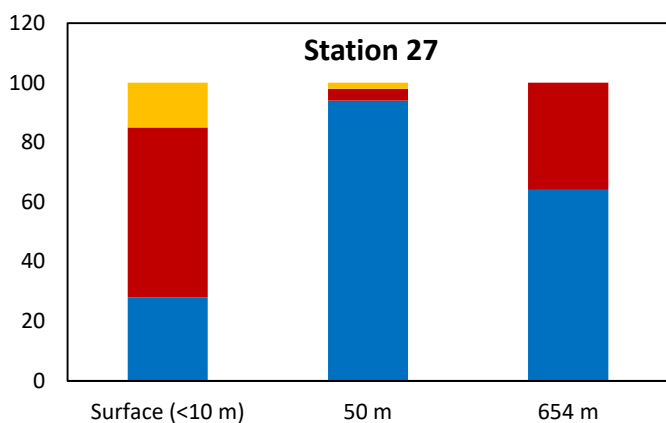
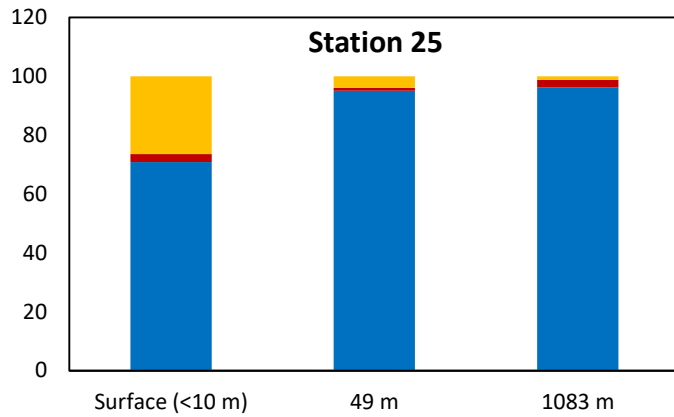
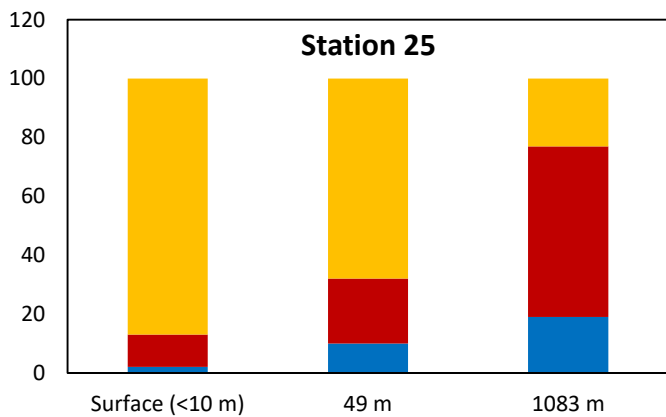
920

921 Figure 7. Conceptual scheme summarizing sedimentation and degradation of ice algae and
922 open water phytoplankton in east Antarctica. Note that in some cases the increase of the
923 ratio IPSO₂₅(1)/HBI III (2) with depth may be due to the faster sedimentation rate of
924 aggregated sympagic algae relative to open water phytoplankton and in other cases to an
925 intense photooxidation (in the euphotic layer) or autoxidation (in the entire water column
926 and in the oxic layer of sediments) of HBI III (2).



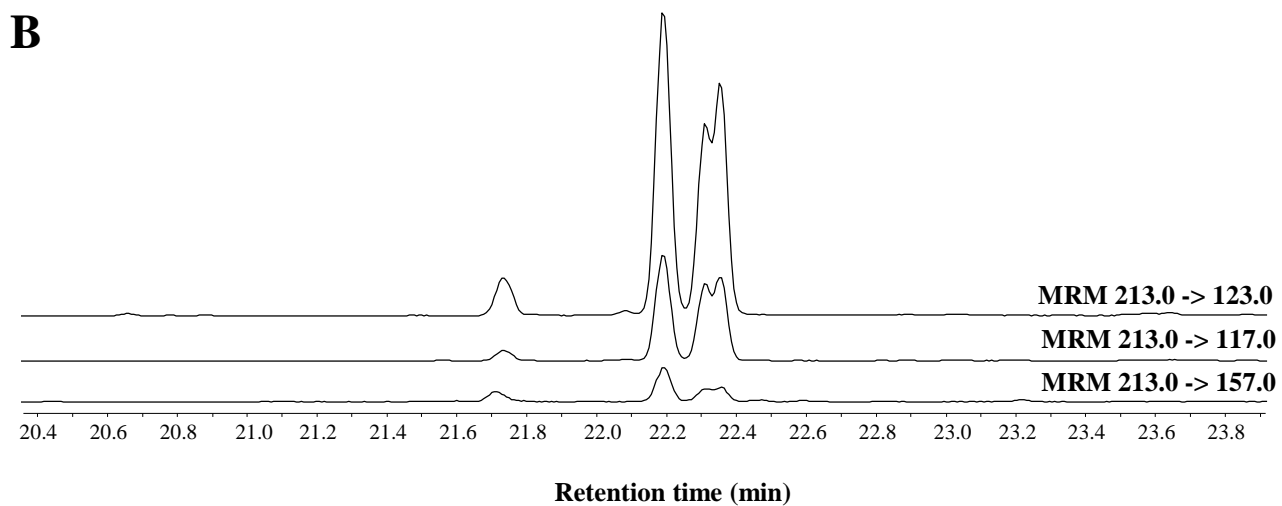
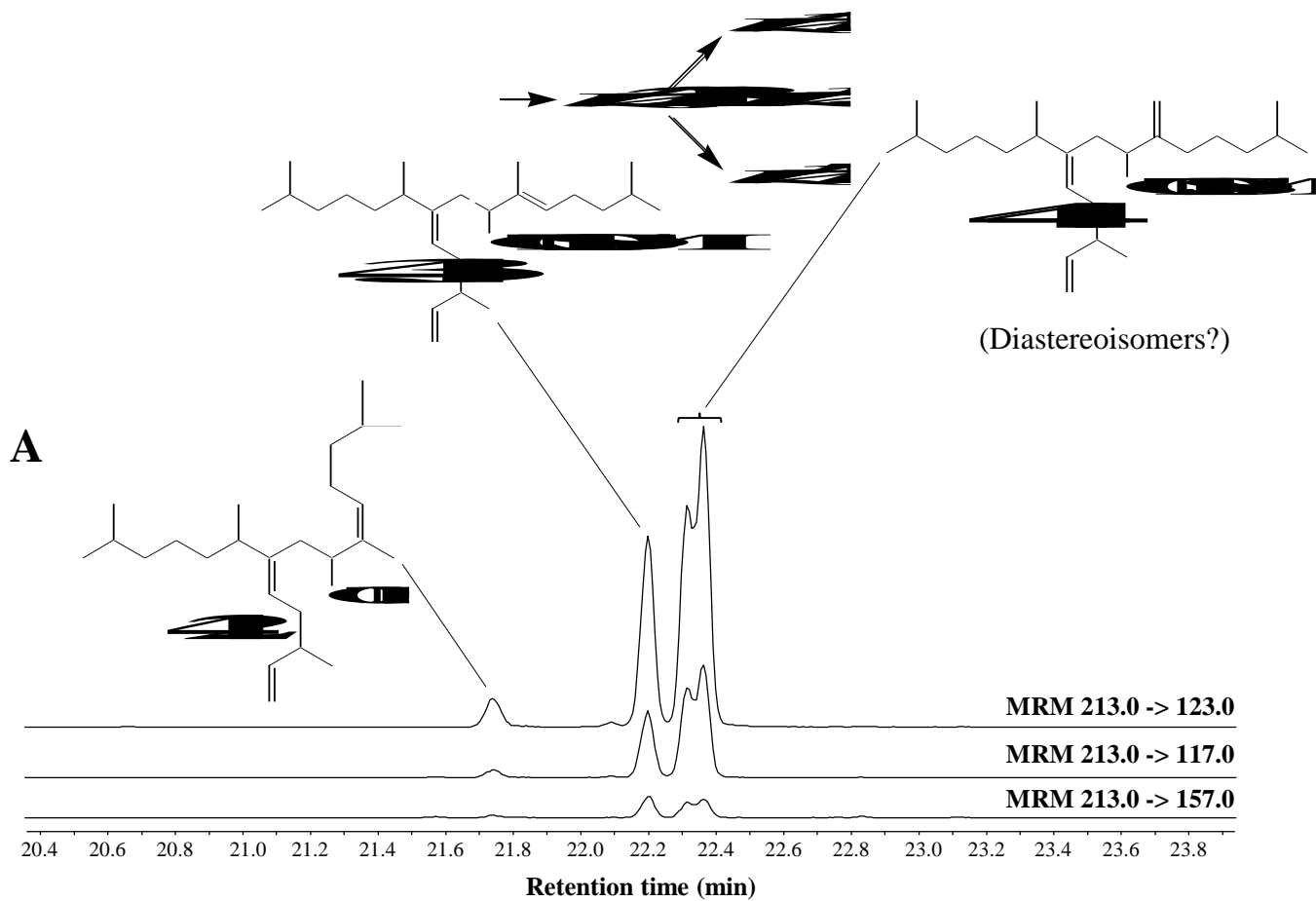
- Detailed lipid analysis (oxidation products)
- Other CTD stations (native lipids only)
- ◆ Sediments (Megacores)

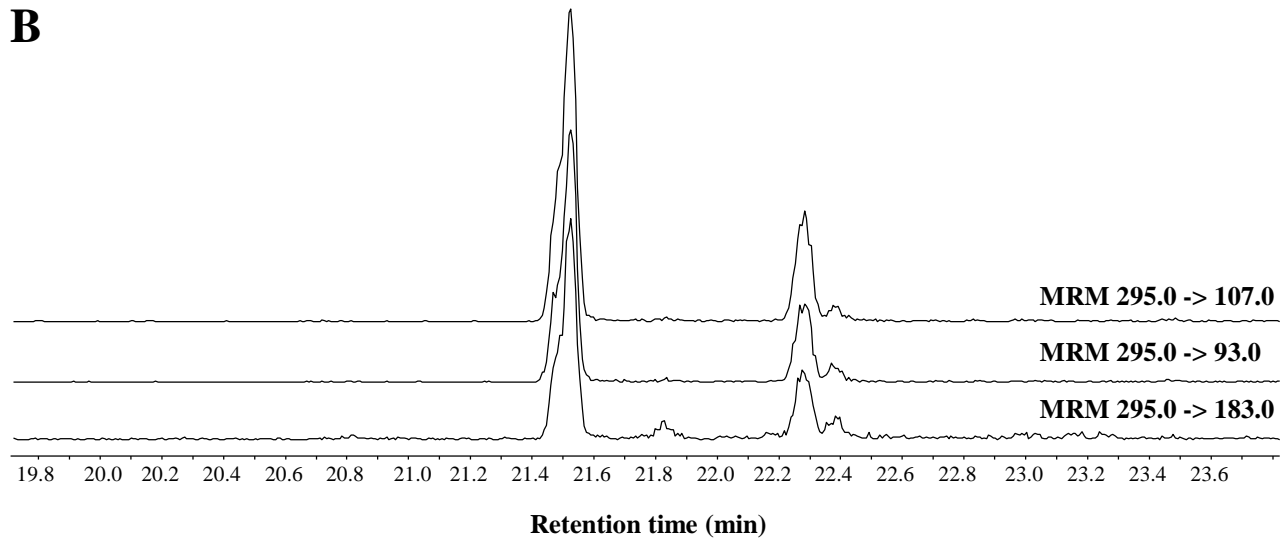
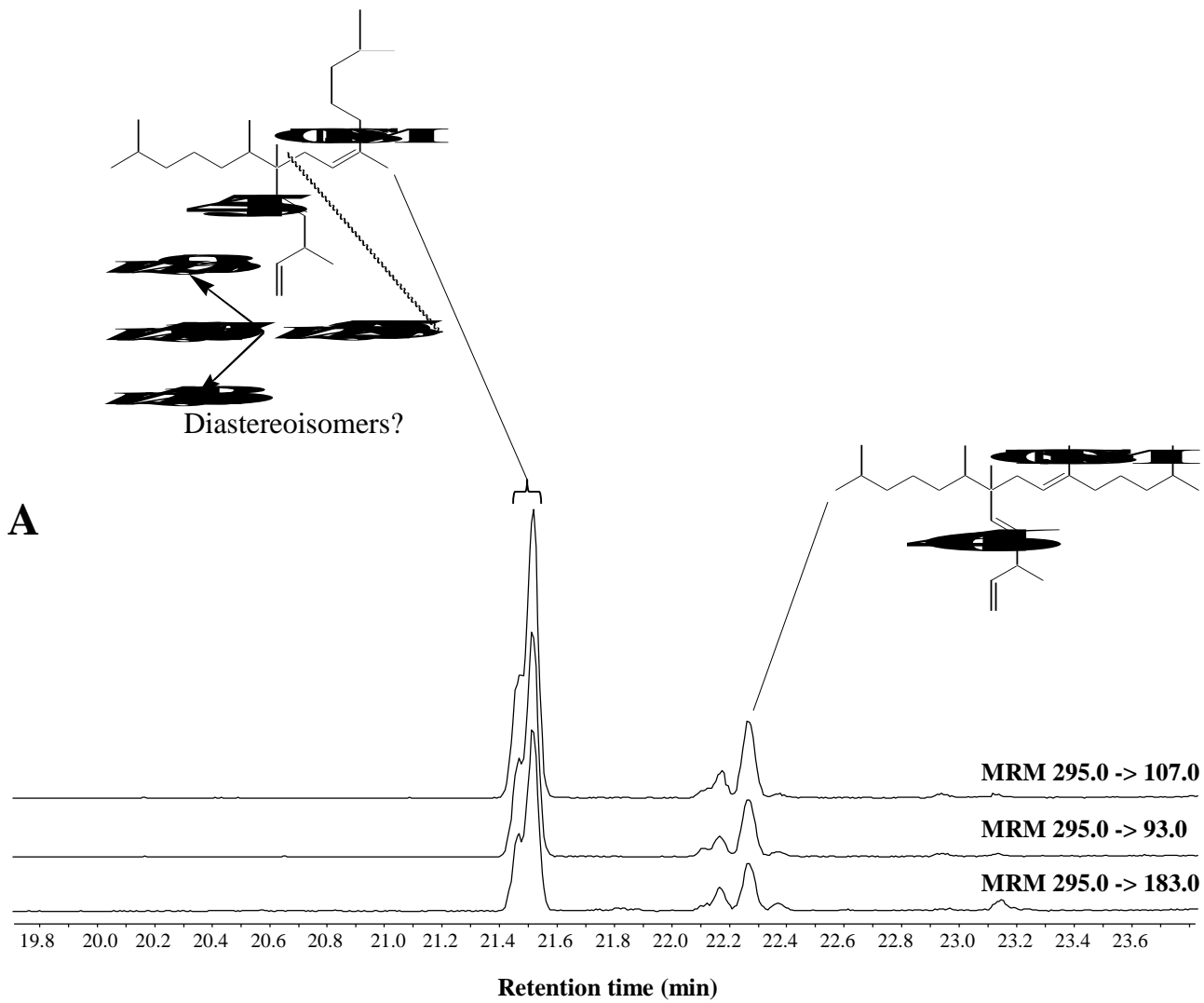


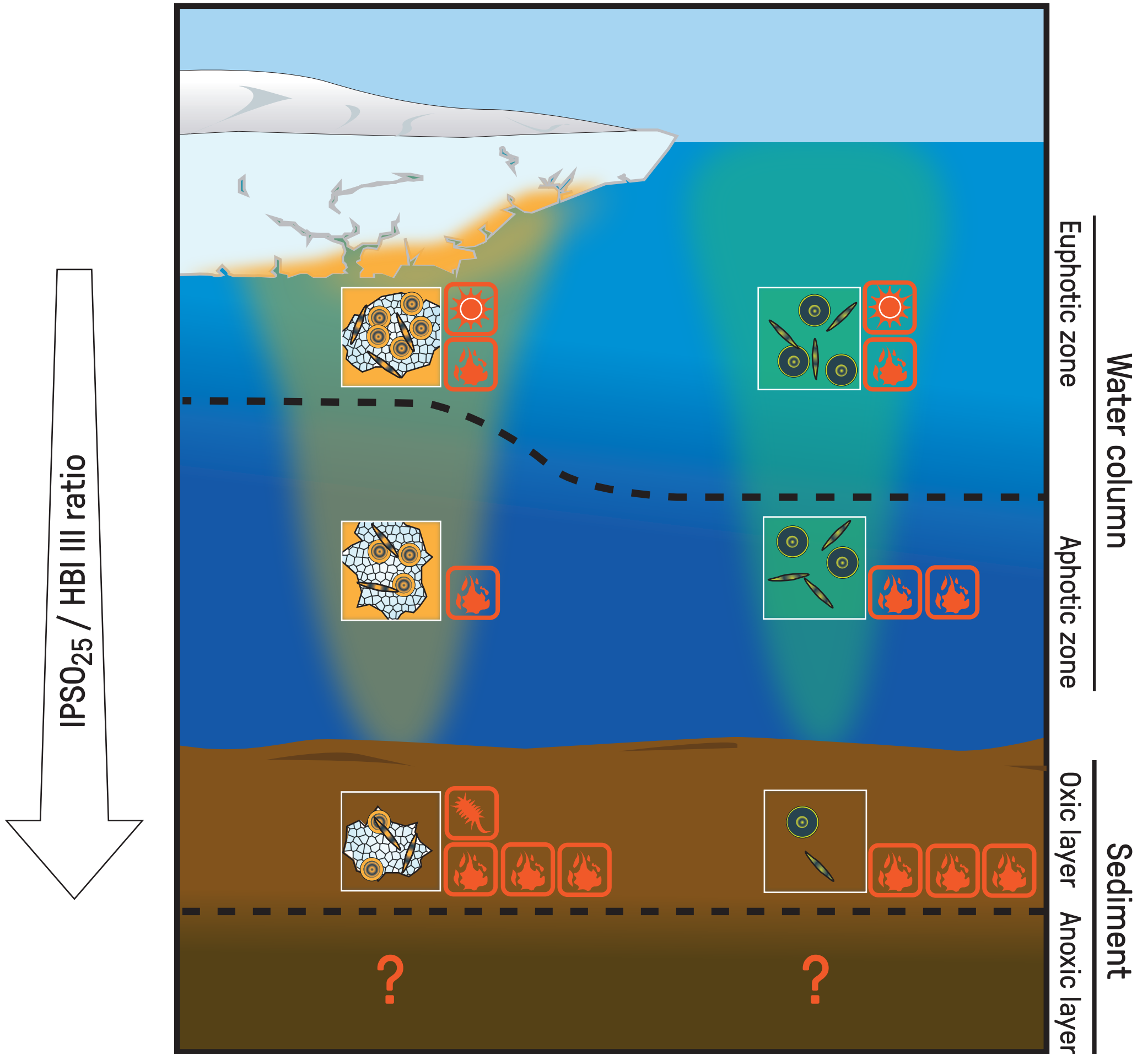


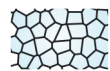
■ Palmitoleic acid ■ Autoxidation ■ Photooxidation

■ Oleic acid ■ Autoxidation ■ Photooxidation







 Extracellular polymeric substances

 Sympagic algae

 Phytoplankton

Degradation pathways:

 Photooxidation

 Autooxidation

 Bacterial

Table 1

Different indicators measured at the five stations selected for lipid degradation analyses.

Station	Depth (m)	IPSO ₂₅ (1)/ HBI III (2)	Cuticular waxes ^a / palmitic acid (24)	<i>Epi</i> -brassicastanol (12)/ <i>epi</i> -brassicasterol (16)	(Palmitoleic acid (23)+ ox ^b)/ palmitic acid (24)	Isophytol (6)/ phytol (4)
25	<10	0.21	0	0.24	30.91	0.45
25	49	0.26	0	0.20	3.42	1.64
25	1083	2.57	0	0.32	1.65	0.60
27	<10	0.26	0.07	0.17	1.82	0
27	50	0.14	2.15	0.21	0.42	0.01
27	654	1.74	0	0.29	0.25	0.08
28B	<10	0.51	0.02	0.14	1.01	0.30
28B	50	0.44	0.03	0.24	3.11	0.06
28B	596	1.61	0	0.16	4.02	0.20
32	<10	0.21	0	0.10	0.05	0.13
32	40	0.37	0	0.09	0.08	0.08
32	563	0.88	0	0.17	0.02	0.07
34	<10	0.25	0.04	0.14	1.11	0.04
34	25	0.21	1.23	0.17	1.10	0.05
34	487	1.54	0	0.28	1.36	0.03

^a Mixtures of 9,16-dihydroxyhexadecanoic (29) and 10,16-dihydroxyhexadecanoic (28) acids

^b Photo- and autoxidation products

Table 2

Comparison of the ratio **1/2** and the autoxidation state of some other algal lipids in SPM and underlying sediments. See Fig. 1 for sample locations.

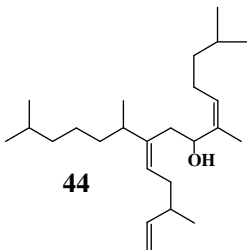
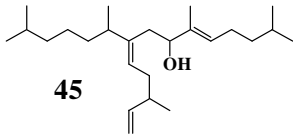
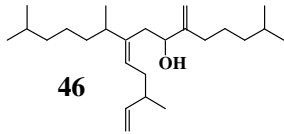
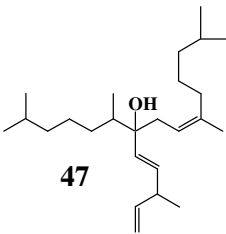
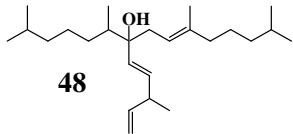
Station – sample type	Depth (m)	IPSO ₂₅ (1)/ HBI III (2)	Sitosterol (42) autoxidation %	Palmitoleic acid (23) autoxidation %	(<i>F. curta</i> + <i>F. cylindrus</i>) / <i>F. kerguelensis</i>
T32 – SPM	<10	0.2	0	1.3	20.6
CTD015 – SPM	40	0.4	0	9.3	18.8
CTD015 – SPM	563	0.9	0	21.8	8.0
MC61 – overlying water	579	1.6	*	*	0.5
MC61 – diatomaceous ‘fluff’	579	2.6	*	*	N/A
MC61 – sediment (1–2 cm)	579	7.5	28.4	53.4	0.7
MC45 – sediment (1–2 cm)	538	11.3	46.3	51.6	0.8

* - not measured

N/A - abundances too low

Table 3

Percentage^a of oxidation products of HBI III (2) detected after NaBH₄-reduction of filtered phytoplankton from Commonwealth Bay (East Antarctica)

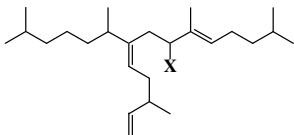
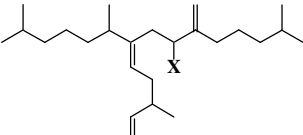
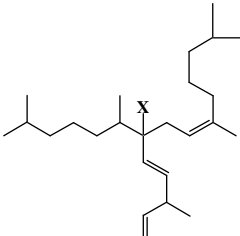
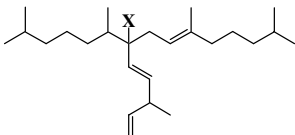
Sample	 44	 45	 46	 47	 48
CB	0.6	9.1	11.2	10.2	5.1
AS607	b	53.4	71.2	65.1	52.7
AS608	10.4	43.6	96.4	9.1	32.7

^a Relative to the residual parent HBI

^b Coelution problem

Table 4

Relative percentages of intact hydroperoxides and their ketonic and alcoholic degradation products measured in the case of the main HBI oxidation products present in phytoplankton from Commonwealth Bay (East Antarctica) (CB sample).

X-				
HO-	18	22	21	45
O=	1	3	-	-
HOO-	81	75	79	55